NATIONAL AERONAUTICS AND SPACE ADMINISTRATION

Technical Memorandum 33-809

A Scanning Laser Rangefinder for a Robotic Vehicle

JET PROPULSION LABORATORY
CALIFORNIA INSTITUTE OF TECHNOLOGY
PASADENA, CALIFORNIA

February 15, 1977

NATIONAL AERONAUTICS AND SPACE ADMINISTRATION

Technical Memorandum 33-809

A Scanning Laser Rangefinder for a Robotic Vehicle

R. A. Lewis
A. R. Johnston

JET PROPULSION LABORATORY
CALIFORNIA INSTITUTE OF TECHNOLOGY
PASADENA, CALIFORNIA

February 15, 1977

PREFACE

The work described in this report was performed by the Control and Energy Conversion Division of the Jet Propulsion Laboratory.

ACKNOWLEDGEMENTS

A number of people have made important contributions to the laser rangefinder we have described in this report. First, Martin Berdahl and Royal Harrison developed and built the low inductance laser pulser which is a vital element of the rangefinder. They described their work in detail in a New Technology Report (Ref. 1) which formed the basis for the laser pulser description herein. Wilbert Hermann designed and built the optical head and skillfully adapted the Surveyor gimballed mirror to our purposes. He also performed the tests which measured the accuracy of pointing the laser beam. Thomas L. Smith developed the early software associated with the rangefinder and carried out various performance tests of the instrument as a whole. The detailed electronic design was ably done by Lee City. In addition, we are grateful to Paul Cassell for assistance in integrating and checking out the electronics, and to Malcolm Rayfield for help in incorporating the rangefinder into the robot system. Robert Cunningham became one of the first users of the LRF system, developing the obstacle mapping procedure described and illustrated in the text.

CONTENTS

CONTENTS (contd)

TABLES

FIGURES

CONTENTS (contd)

ABSTRACT

A scanning Laser Rangefinder (LRF) which operates in conjunction with a minicomputer as part of a robotic vehicle is described. The description, in sufficient detail for replication, modification and maintenance, includes both hardware and software. Also included is a discussion of our functional requirements relative to the state-of-the-art; a detailing of the instrument and its performance; a summary of the robot system in which the LRF functions; the software organization, interfaces and description; and the applications to which the LRF has been put.

I. INTRODUCTION

This document as a whole is intended to provide the information necessary for the replication, modification, maintenance, and use of the Laser Rangefinder (LRF) system. The introductory section directs its attention to the historical and technical context in which the present laser has been developed. Section II describes the existing laser instrument. The Robot system in which it functions and some of the pertinent interfaces are briefly described in section III. Section IV focuses on the software organization, and examples of LRF applications and performance are given in section V. Finally, the limitations and possible improvements to the rangefinder are described in section VI. Further details of the instrument design and of the software organization are contained in the Appendices.

Development of the instrument described in this report was begun in 1972 as a part of a continuing Robot Research Program at the Jet Propulsion Laboratory (Ref. 2). The Program is concerned with techniques for moving a vehicle about at a remote location and accomplishing useful tasks autonomously, without detailed human interaction. The tasks of interest include location and manipulation of rock samples on the surface of a planet.

The motivation for development of the LRF was to provide a means for geometrical, three-dimensional location of objects or surfaces in the neighborhood of the robot vehicle for use as input information to the autonomous control system. The LRF instrument was a part of a "vision" system that included two television cameras and a **minicomputer.** The relationship of the LRF to the robot system as a whole is discussed further in a later section.

The most important problem initially addressed was that of locating a rock-like object for grasping by a manipulator. A second problem, which is just beginning to receive attention, is that of obstacle detection or terrain mapping for use during vehicle motion. These applications shaped the performance requirements for LRF instrument.

The robot vehicle system required the LRF to be interfaced directly with a computer, to accept instructions from the computer, and read output data into it for subsequent processing.

The instrument beam must be directed at specified points or scanned over a specified area under computer control. The manipulator hand is roughly the size of a human hand, so a capability to determine the position of a target within a few centimeters was desired. This accuracy is needed over a region extending roughly from 1 meter to 3 meters range. In addition, ranging with good repeatability to 30 to 50 meters but without the centimeter accuracy requirement was needed for vehicle motion inputs. A capability for outdoor operation in full sunlight was also required. Reasonably fast operation such that the overall function of the robot would not be slowed while waiting for data was also important, but no hard requirement for exceeding a critical data rate was envisioned.

Finally, since the ultimate application was to a planetary rover, a technique which could ultimately result in a reasonably small and rugged package was needed.

Many rangefinding instruments have been developed, both with better accuracy and with longer maximum range capability than we needed. A list of some of these is given in Appendix A for reference. However, no existing instrument could be found that would do the entire job.

Early laser-distance measuring devices employed a continuously emitting (CW) laser together with a modulator (Ref. 3), or even a mercury arc lamp and modulator (Ref. 4). The modulation was typically at 10-50 Mhz, and phase-determining electronics extracted the desired distance data.

Alternatively, a pulsed light source was used (Refs. 5, 6), and the range was determined from a measurement of the round-trip return time of the light pulse.

The CW form of optical rangefinder has been developed in recent years into sophisticated and compact instruments used for surveying (Ref. 7), with accuracies in the few mm range, and also for ground-surface profiling from

aircraft (Ref. 8). Introduction of a light-emitting diode (LED) as the light source greatly simplified the device and brought about an all-solid state instrument (Ref. 7). However, the intensity of an LED source is low and does not permit measurement directly off of a rough surface at tens of meters. The surveying instruments are designed to operate with a retroreflector target, which increases the intensity of the reflected return by many orders of magnitude.

The pulsed type of ranger was also developed, mostly by the military, into compact, high intensity instruments capable of ranging to many km distance (Refs. 9, 10, 11). However, the duration of the light pulse has typically limited accuracy to the order of 1 meter. Similar instruments were also developed by NASA (Refs. 12, 13) for ranging from the lunar orbiter to the moon's surface.

In further developments, solid state GaAs lasers were used in pulsed time-of-flight rangefinders at distances of roughly 75 m by Kelley and Reynolds at NASA's Johnson Space Center (Ref. 14). They observed repeatability to within about 30cm, which approached our goal. Subsequently, the work of Shumate at JPL, reported in a study relating to optical ground station location using a satellite target (Ref. 15), showed that a robot LRF using a solid state pulsed laser was possible. He obtained a measurement precision of roughly 2 cm.

Other robot projects have also developed ranging instruments, one a short-range CW LED device (Ref. 16) and another based on a CW HeNe Laser (Ref. 17). Herzog (Ref. 18) has described a sophisticated system for accurate laser ranging which combines features of both pulse and CW systems.

It was felt for our application that a solid-state laser rather than an LED source was desirable in order to ensure a future capability of operating at distances exceeding 30m. With such a laser, pulsed operation is necessary for thermal reasons. Averaging of the time-of-flight measurement over many light pulses was incorporated in the instrument in order to reduce the inevitable noise in the data to a reasonable level. Averaging of the pulse travel time

is analogous to the heavy output filtering typical on CW phase-type instruments. The shorter the rise time of the light pulse for a given output light power the greater the potential measurement accuracy. The best form of light pulse would therefore be a delta function spike. Our present light source has a relatively slow rise time, so we anticipate that a significant improvement in overall accuracy could result from shortening the light pulse.

These, then, were the technical constraints and requirements for the instrument described in the following section.

II. INSTRUMENT DESCRIPTION AND PERFORMANCE

This section describes the Laser Rangefinder (LRF) hardware and discusses the main factors affecting the instrument's performance.

A. Instrument Description

Physically, the LRF consists of two packages: (1) an optical head containing the light source, photo-detector, and means for forming and pointing the beam, and (2) an electronics package containing the control and measurement circuits. A photograph of the complete instrument is shown in Fig. 2-1 in a laboratory setting.

An overall block diagram of the LRF is presented in Fig. 2-2. The laser light is a gallium aluminum arsenide solid-state laser. A clock, not shown in Fig. 2-2, drives the laser pulser at a 10 kHz rate and also provides timing for related functions. The detector is a type C31034 photomultiplier having a gallium arsenide photo surface with spectral sensitivity to match the laser emission (Ref. 19). A GaAlAs laser operating near 0.84μm was selected rather than a GaAs type emitting at 0.90μm because the photomultiplier cathode efficiency drops off very rapidly at wavelengths approaching 0.9μ.

The constant-amplitude current pulse used to drive the laser is sampled at the pulser by an inductive loop and is used as the timing reference for measurement of the light pulse time-of-flight. The photomultiplier output pulse, generated by the reflected light, is of variable amplitude, depending on the nature of the surface of interest and the range to be measured. As a result, a module called a constant fraction discriminator (Fig. 2-2) is introduced to minimize the effect of reflected light pulse amplitude on the range measurement.

The time interval measurement itself is made by a time-to-pulse-height converter (Ref. 20), a module which produces a relatively long (2 microsecond) output pulse for each start-stop pulse pair accepted. The amplitude of this output pulse is accurately proportional to the start-stop time interval, and is subsequently sampled, averaged over many pulses, and converted to a digital

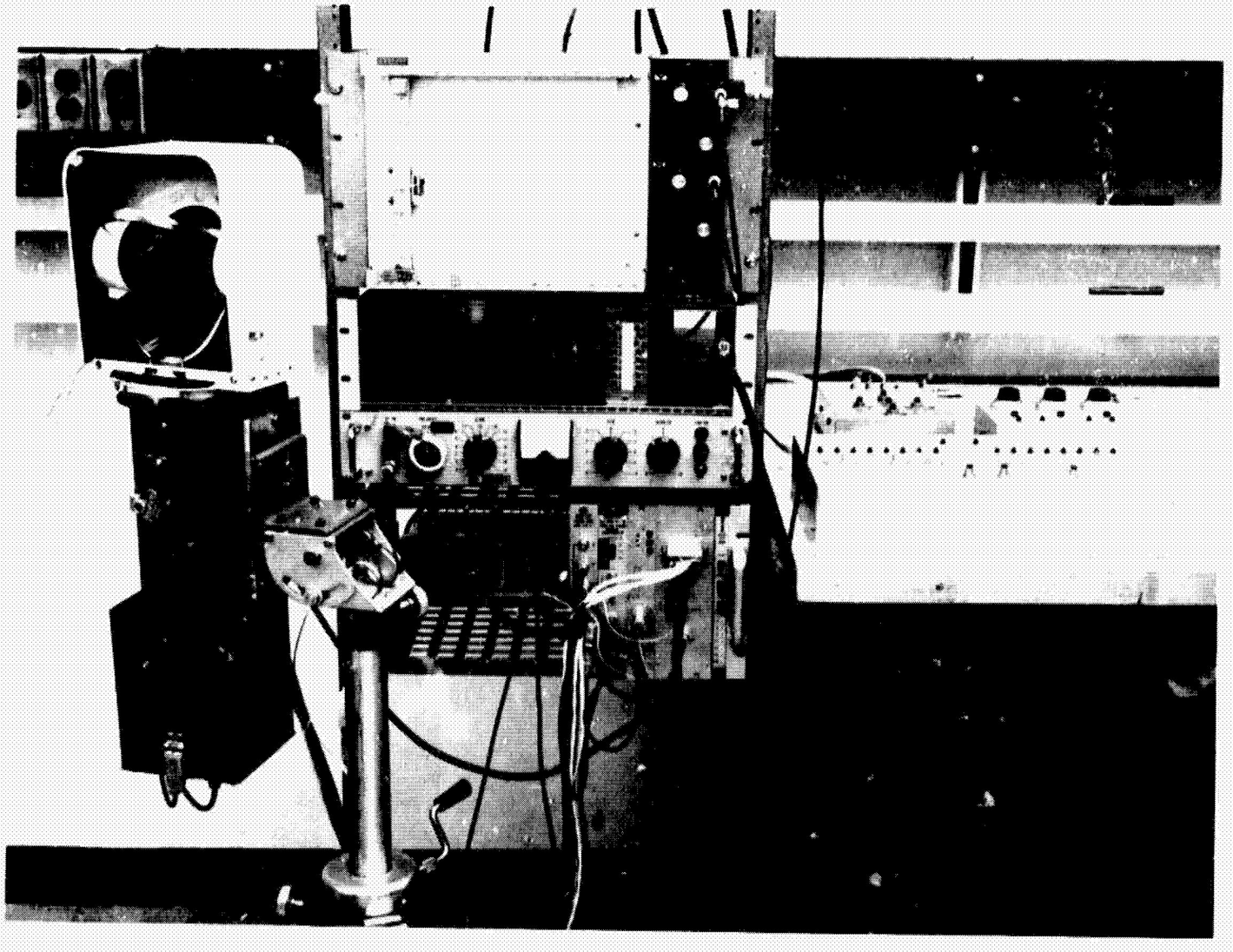

Figure 2-1. LRF Instrument in Laboratory Setting

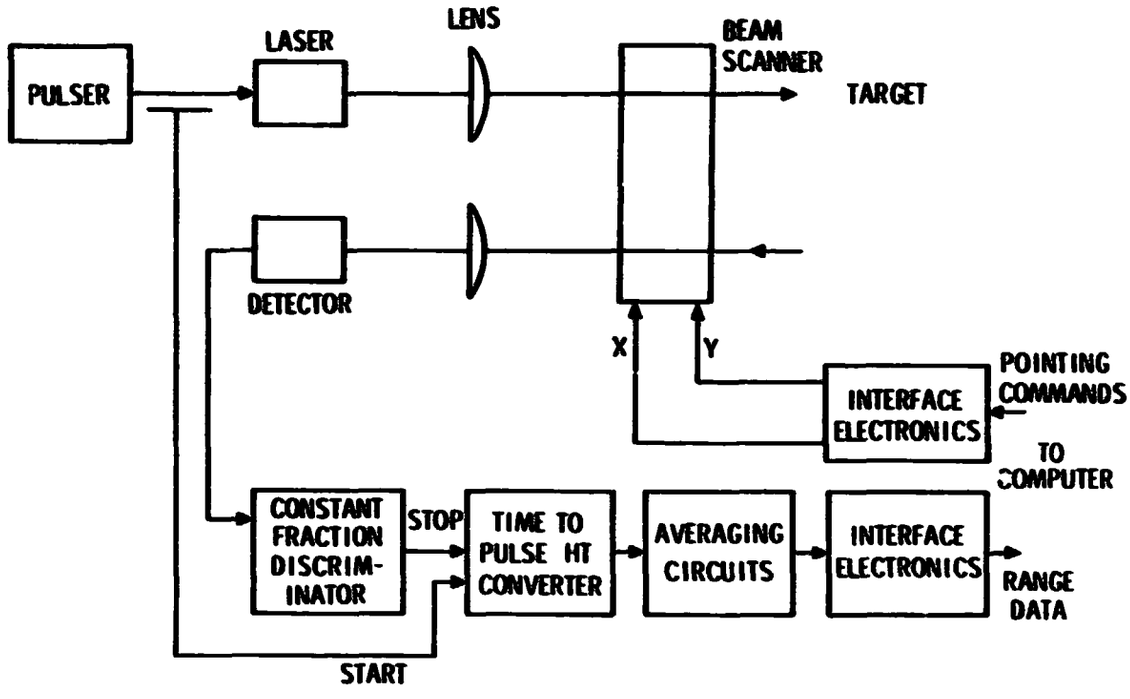

Figure 2-2. Block Diagram of the Laser Rangefinder

form for transmission to the computer which interfaces in real time with the LRF instrument. Both critical elements in the time interval measurement process, the constant-fraction discriminator and the time-to-pulse-height converter, are commercial nuclear physics instrumentation.

Computer, a General Automation SPC 16-85, also supplies pointing commands which are used to drive the beam scanner. The scanner is a gimballed mirror driven by stepper motors in elevation and azimuth. The single mirror reflects both transmitted and received light beams, but there are separate, non-overlapping transmitter and receiver apertures.

B. Instrument Operation

Although the time-to-pulse-height conversion is sufficiently linear for our purposes without further improvement, slow electronics drifts would limit the accuracy of the LRF. In order to eliminate the effects of these drifts and permit object location to roughly one centimeter, a self-calibration procedure

has been incorporated. This procedure is equivalent to operating the instrument in a comparison mode in which an unknown position is determined relative to a known target. As a result, LRF range data is not affected by slow delay-time drift in any component.

Note that the time interval between start and stop pulse includes contributions from component delays and internal cable transit times. These delays add up to 50 to 100 ns total, compared to the light time-of-flight of approximately 20 ns at a 3 m range. The start pulse cable length is adjusted so that the start-stop pulse interval is close to the actual light pulse travel time. There is no zero distance reference inherent in the instrument. Measurements could be made down to zero range (target in plane of LRF mirror) with appropriate cable trimming, but actually the instrument was set up with a minimum range of approximately 1 m.

Errors due to reflectivity variations remain. Care must be taken to optimize the effectiveness of the constant fraction discriminator, but the system presently runs open loop with respect to reflectivity. In principle, the self-calibration procedure could be expanded to involve reflectivity, but only at the cost of increased complexity.

The self-calibration procedure has been implemented by placing two test targets as known positions on the rover vehicle and performing a range measurement from each at selected times during LRF operation. The calibration data is then used to calculate a scale factor and bias for converting laser output voltage into absolute range. The two test targets are placed near the closest and furthest ranges to be expected during a manipulation, 1 m and 2.5 m.

Although two test targets are used, one calibration target placed at an average manipulation distance would suffice, since drift in scale factor is small.

A second operational requirement, called "reset," is concerned with matching the actual mirror step position with its corresponding digital representation.

Mirror positioning is an incremental process, and no step-by-step feedback is present to measure mirror position; the position control system is implemented entirely in the electronics. The reset operation must be done at turn-on time. Normally, no subsequent reset is required until the system is shut down, the mirror being moved one step at a time while the mirror position register is simultaneously incremented.

The reset command indexes the mirror to a predetermined position, determined by linear potentiometers on the mirror azimuth and elevation axes, while simultaneously loading the mirror position register with the correct step number. After the reset is executed, the same potentiometers are used to monitor mirror position during operation, and if a discrepancy between actual mirror position and the position register occurs, an error ("skip-step") is signalled. The reset operation must be repeated after such an error.

C. Rangefinder Performance

As indicated above, the LRF measurement is a relative one in which target position is compared to the known position of a calibration target. Such a scheme is analogous to chopper stabilization of a dc amplifier. It is not necessary to alternate the calibration target and the unknown; the drifts are slow enough that a recalibration every five minutes is sufficient. thout using a comparison technique, temperature-dependent range bias drift on the order of 30 to 50 cm could be expected. The drift is concentrated during a warmup period of 10-15 minutes.

The dominant error source for the range measurement is caused by the unknown reflectivity of the target, which results in a varying amplitude of the reflected light pulse. Angle of incidence also contributes to the intensity variations.

Measurement to an unknown target within 2 cm or better is possible with care. Unexpectedly small reflected light intensity (as from a very black target) will cause larger errors. Adjustment of the constant-fraction discriminator is important, and must be maintained, although it has been found to be stable over periods of many days. Perturbation of the shape of the photomultiplier pulse

by cross-talk or ringing must be avoided in order to maintain stable discriminator performance.

The errors caused by reflectivity variation, called "walk," are not fundamental in nature but are repeatable. They can be reduced by shortening the light pulse rise time, and can also be reduced if a better type of intensity-independent discriminator could be developed. Candidates for testing (Ref. 21) exist, but to date they have not been investigated. Walk error could also be reduced by monitoring the intensity of the return light pulse and using it to compute a range correction.

A visual representation of relectivity errors, caused in part by an imperfectly adjusted constant fraction discriminator, is provided in Figs. 2-3 and 2-4. The latter figure is a range picture (LRF output expressed as intensity data on a video monitor) of the test pattern shown in the former figure. A "perfect" instrument would yield a uniformly gray rangepic, whereas in fact the test pattern's variations are reproduced all too faithfully by the LRF. Even so, the instrument is useful in a wide variety of applications (Section V).

The second type of ranging error, caused by electronic noise, is presently much smaller than the reflectivity walk error, but can become significant if a high data rate (approaching, for instance, 100 points per second at a 2m range) is required.

Experimental data summarizing the accuracy of the present instrument are given in Appendix B.

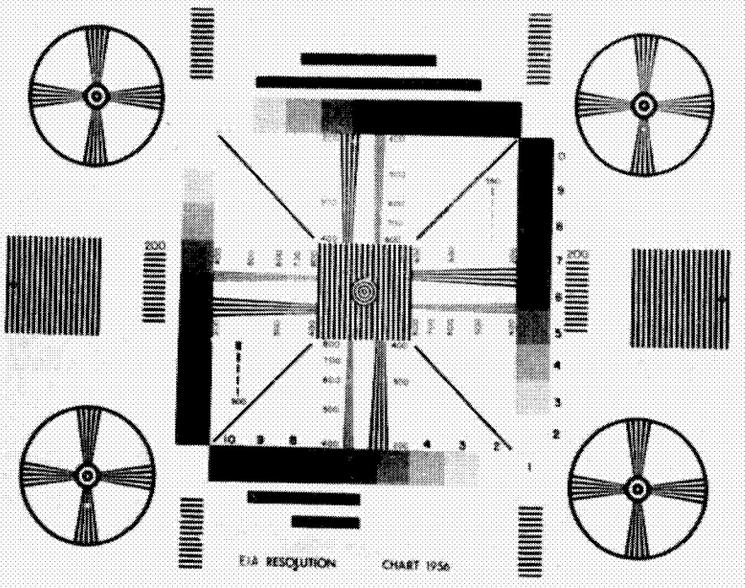

Figure 2-3. Test Pattern

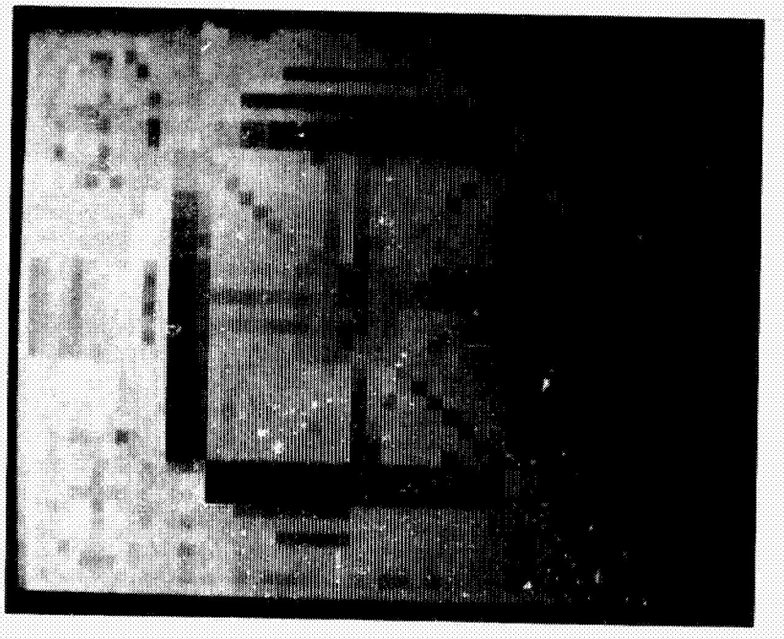

Figure 2-4. Rangepic of Test Pattern

III. ASSOCIATED ROBOT SYSTEM

The performance evaluation criteria, LRF software organization, and applications to which the LRF is put are all dependent upon the context in which the instrument functions. The scanning laser instrument described in the previous section is embedded in a robot system. In this section, the robot system is described, with emphasis placed on those aspects interacting in some way with the LRF. A brief description of coordinate frames relevant to LRF operation is then given, followed by a summary of system-induced errors impacting LRF performance.

A. Robot Description

The robot (Figs. 3-1 and 3-2) has been designed as an integrated set of environmental sensors and effectors. The system is a breadboard, intended to provide a tool for testing various approaches to problem-solving and autonomous operation. The long-range conceptual goal is an autonomous Martian roving vehicle able to make independent decisions, gather the information required to make those decisions, and act on those decisions, all in a manner consonant with broad mission goals. The major components are locomotion, manipulation, and perception (vision) systems.

The locomotion system consists of a large (1.5 m x 3 m) flat vehicle with four independently-driven wheel drive and steering motors, two odometers and a gyrocompass, and the associated software. Except for the computers (a remote timeshared Decsystem 10 and a dedicated resident General Automation SPC 16-85), all robot hardware is mounted on the vehicle. Power and data are provided by umbilical. The vehicle is capable of (tethered) outdoor operation. LRF data is used by the path planning software in the generation of obstacle maps before the vehicle moves, and during motion in providing a safety function.

The manipulator system consists of a six degree-of-freedom modified Stanford Electric Arm, designed for computer control, and the associated software. The manipulator (Ref. 22) is mounted on the vehicle bed, 45 cm above the ground surface. It has binary tactile sensors mounted on the parallel jaw fingers, a wrist-mounted force/torque sensor, and two proximity sensors (one on each finger). The arm-mounted proximity sensors (Ref. 23) are capable of providing,

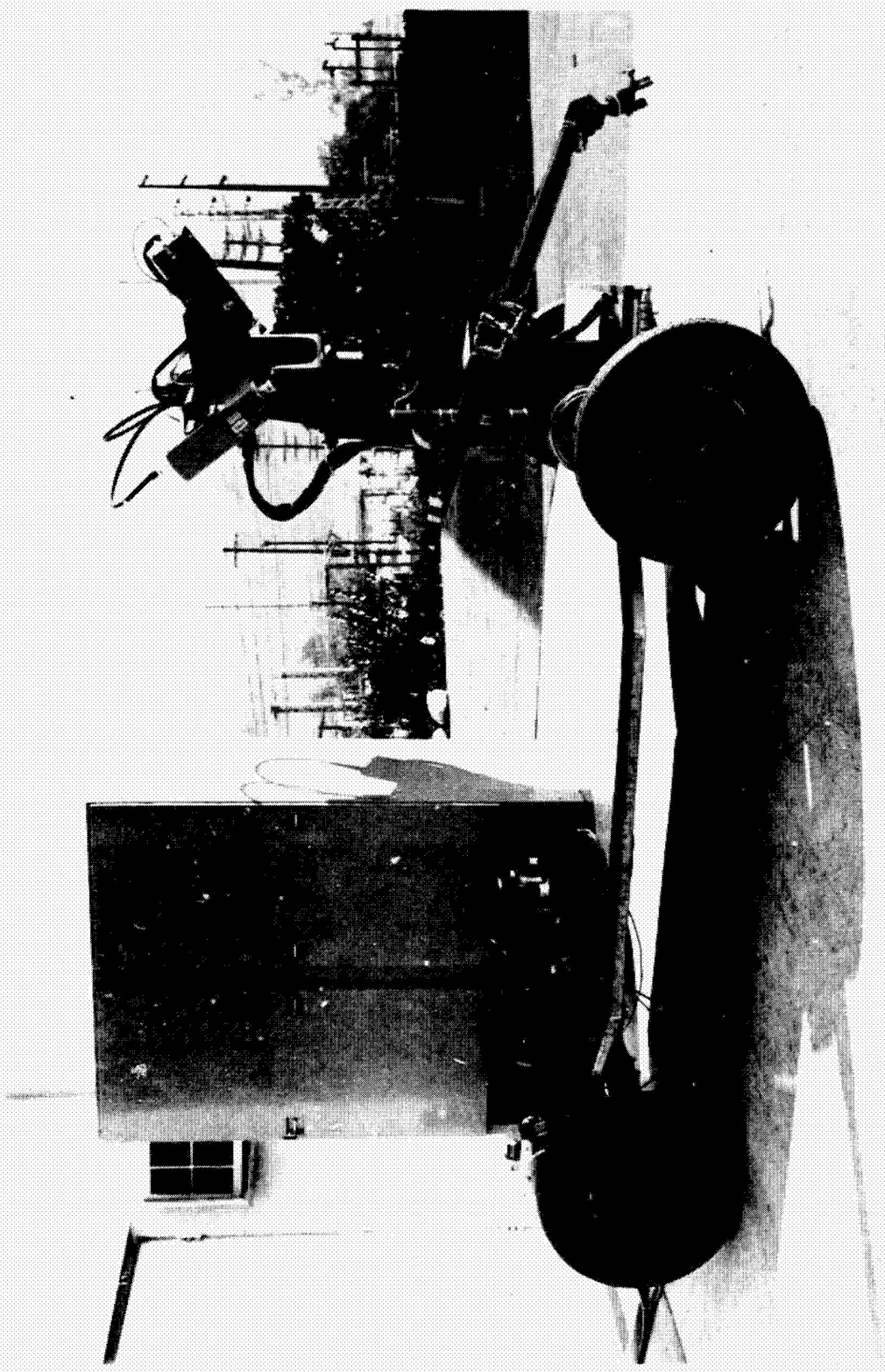

Figure 3-1. JPL Research Robot

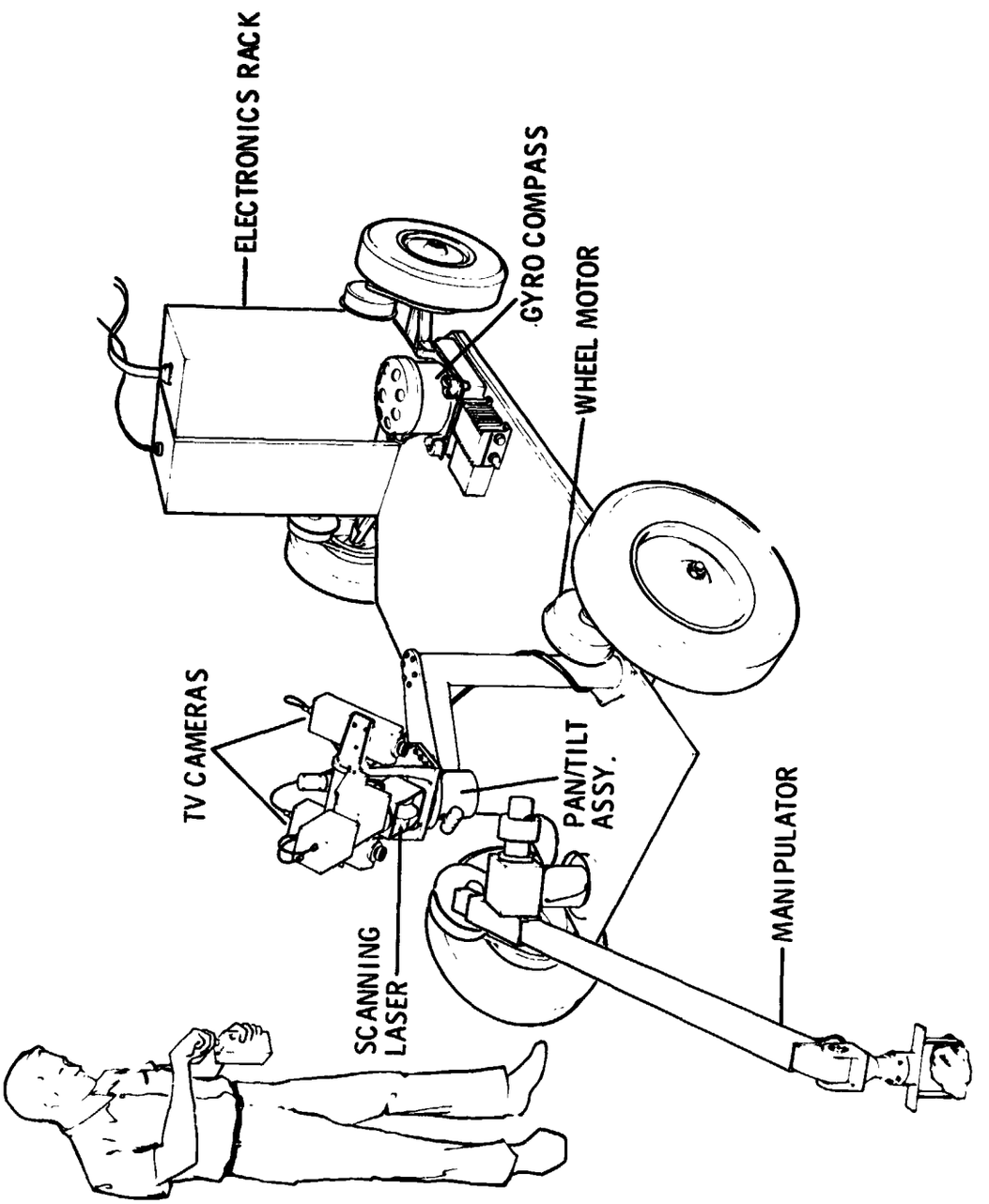

Figure 3-2. Sketch of JPL Research Robot

within a domain limited by where the arm can move, information of the same sort provided by the LRF. Thus a potential redundancy between the LRF and proximity sensors exists. LRF data on object and obstacle location can be directly used by the manipulator software.

The perception system proper includes the LRF, two TV cameras, and associated software, and excludes sensors that provide only indirect information about the environment (e.g., motor current monitoring which can yield slope information, arm error torques which can yield weight, and proximity sensors). The cameras and LRF are mounted on a common pan-tilt head, approximately 1.2 m above the surface of the vehicle. The basic task of the perception system is the detecting, recognizing, and locating of objects of interest and obstacles to vehicle and manipulator motion. The dual TV cameras and the LRF combine to provide much redundant information. Various ways of optimizing the usefulness of the redundancy are currently being investigated.

B. Coordinate Frames

There are three coordinate frames relevant to laser operation (Fig. 3-3). One, the ARM system, is centered at the base of the manipulator, on the vehicle surface. The unit vectors of the ARM system point, respectively, across the vehicle front ($\vec{X}_A$), in the direction of forward vehicle motion ($\vec{Y}_A$), and up from the vehicle surface ($\vec{Z}_A$).

A second coordinate frame is the rotated pan-tilt (RPT) system. Its three axes ($\vec{X}_R$, $\vec{Y}_R$, $\vec{Z}_R$) are aligned with the pan-tilt head's present (rotated) position and point, respectively. along the line of sight, tilt axis, and pan axis. This frame is centered at the laser, at the point where the beam would intersect the LRF mirror when the instrument is at the "reset position." The reset position is the LRF azimuth/elevation setting that directs the beam along the line of sight of the pan-tilt head, the so-called "straight ahead" position.

If a vector in ARM coordinates is represented by

$$\vec{V}_A = (X_A, Y_A, Z_A, 1)^T$$

and a vector in RPT coordinates by

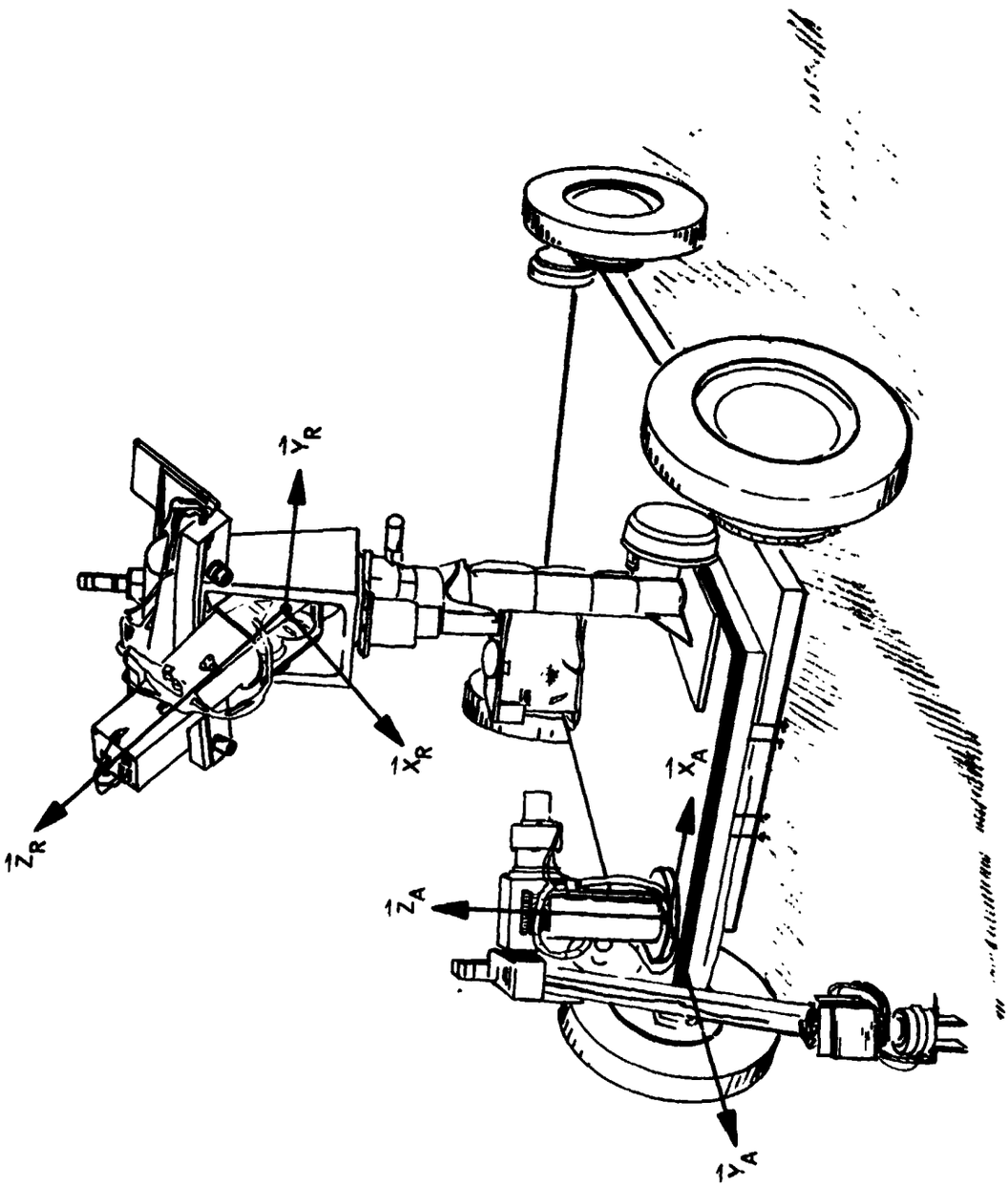

Figure 3-3. LRF and Arm-Based Coordinate Systems

$$\vec{V}_R = (X_R, Y_R, Z_R, 1)^T,$$

then the two systems are related by

$$\vec{V}_A = T_A^R (\vec{V}_R + \vec{D}_R) \qquad \text{and} \qquad \vec{V}_R = T_R^A \vec{V}_A - \vec{D}_R,$$

where $\vec{D}_R = [20.32, 0, -11.68, 0]^T$, a constant displacement vector of the LRF from the pan-tilt center, in centimeters, and

$$T_A^R = \begin{bmatrix} S_\phi C_\theta & C_\phi & S_\phi S_\theta & 81.28 \\ -C_\phi C_\theta & S_\phi & -C_\phi S_\theta & 7.62 \\ -S_\theta & 0 & C_\theta & 130.81 \\ 0 & 0 & 0 & 1 \end{bmatrix}$$

The subscripts in the elements of T_A^R refer to the pan (ϕ) and tilt (θ) angles of the pan-tilt head, the "S" and "C" to sines and cosines of these angles.

The inverse matrix T_R^A is given by

$$T_R^A = T_A^{R\,-1} = \begin{bmatrix} S_\phi C_\theta & -C_\phi C_\theta & -S_\theta & -81.28 S_\phi C_\theta + 7.62 C_\phi C_\theta + 130.81 S_\theta \\ C_\phi & S_\phi & 0 & -81.28 C_\phi - 7.62 S_\phi \\ S_\phi S_\theta & -C_\phi S_\theta & C_\theta & -81.28 S_\phi S_\theta + 7.62 C_\phi S_\theta - 130.81 C_\theta \\ 0 & 0 & 0 & 1 \end{bmatrix}$$

The third coordinate frame is the laser step (LST) system, centered at the reset position's beam-mirror intersection point. It is linearly related to a spherical system, its first two "axes" being integer stepper-motor step numbers related to azimuth (α) and elevation (ε), respectively, and its third axis being a range number (r) equivalent to the time of flight to target. If a vector in the LST system is represented by

$$\vec{V}_L = (\alpha, \varepsilon, r, 1)^T,$$

then the azimuth angle α', elevation angle ε' (both in degrees), and actual range r' (in centimeters) are given by

$$\vec{V}_L' = (\alpha', \varepsilon', r', 1)^T = T_L^L \cdot \vec{V}_L,$$

where

$$T_{L'}^{L} = \begin{bmatrix} -0.3095 & 0 & 0 & 225.9569 \\ 0 & 0.3307 & 0 & -244.0418 \\ 0 & 0 & a & b \\ 0 & 0 & 0 & 1 \end{bmatrix}$$

The entries "a" and "b" are the results of the laser calibration process referred to in the preceding section and described in the next one.

The LST and RPT system are related by the following:

$$\vec{V}_R = \begin{bmatrix} X_R \\ Y_R \\ Z_R \\ 1 \end{bmatrix} = \begin{bmatrix} r' \cos\varepsilon' \cos\alpha' \\ -r' \cos\varepsilon' \sin\alpha' \\ -r' \sin\varepsilon' \\ 1 \end{bmatrix}$$

Inversely, to transform from RPT to LST,

$$\vec{V}_{L'} = \begin{bmatrix} \alpha' \\ \varepsilon' \\ r' \\ 1 \end{bmatrix} = \begin{bmatrix} \tan^{-1}\left(-Y_R/X_R\right) \\ \tan^{-1}\left(-Z_R \Big/ \sqrt{X_R^2 + Y_R^2}\right) \\ \sqrt{X_R^2 + Y_R^2 + Z_R^2} \\ 1 \end{bmatrix}$$

and $\vec{V}_L = T_L^{L'} \vec{V}_{L'}$, where

$$T_L^{L'} = \left(T_{L'}^{L}\right)^{-1} = \begin{bmatrix} -3.2310 & 0 & 0 & 730 \\ 0 & 3.0241 & 0 & 738 \\ 0 & 0 & 1/a & -b/a \\ 0 & 0 & 0 & 1 \end{bmatrix}$$

The domain of laser operation, in LST coordinates, is $\alpha \in [31, 1023]$, $\varepsilon \in [100, 857]$, and $r \in [0, 1023]$. At $\alpha = 730$, $\varepsilon = 738$, the beam points straight ahead along the pan-tilt assembly line of sight, $\vec{X}_R$.

C. System-Related Effects Impacting LRF Performance

There are three major components to any evaluation of the LRF as it performs in the total robot system. These are vehicle-relative pointing accuracy, ranging accuracy, and external environment-relative factors.

It has been found that the laser beam can be pointed with both precision and very high degree of repeatability relative to the vehicle. This is due in part to the fact that the beam cannot "rest" anywhere in its two-dimensional (azimuth, elevation) space, but only at the lattice points dictated by the incremental nature of the stepper motors. The pan-tilt head on which the laser is mounted is likewise an incremental precisely repeatable subsystem. Thus it is that the beam can be repeatedly directed in the same physical direction whenever the four pointing variables (ϕ, θ, α, ε) are repeated by command. This, of course, is one of the features enabling the recalibration

process to function smoothly; the beam can reliably be directed to the same target points.

Determination of the beam direction, even relative to the vehicle, is not quite as precise. The positioning of the pan-tilt head, its alignment with the vehicle frame, and the orientation of the LRF azimuth and elevation axes relative to the pan-tilt assembly are only estimated, though to within a high angular tolerance. In particular, the "zero" pointing direction (pointing the beam in the direction of vehicle motion, parallel to the frame) is perhaps accurate only to an estimated half degree.

Another source of beam pointing error is vehicle sag. The platform on which the arm, pan-tilt (including cameras and laser), and electronics rack are mounted is a somewhat flexible frame. The platform sags slightly, to varying degrees and in varying directions at different locations, thus affecting beam pointing.

Ranging inaccuracies have been described in an earlier section. Suffice it to say here that the net effect of errors in ranging is an inaccuracy in position estimates along the line of sight.

These error sources all affect the determination of position of an object in the environment. For precise position determination, all of the parameters of the transformations given above must be known. Slight errors in estimating displacements between the arm and pan-tilt and also along the pan-tilt to the laser, as well as errors in ranging and pointing (due largely to vehicle sag) all effect the accuracy to which an object in the external environment can be sensed.

As the applications presented in Section V show, however, even with all these sources of error, significant use of the instrument can be and has been made.

IV. SOFTWARE DESCRIPTION, ORGANIZATION, AND USER INTERFACES

The primary function of the laser software is to move the laser to a specified point and then take a range reading. Moving the laser beam involves controlling the laser scan apparatus, picking a mode (scan several points and take readings, or slew to one point and take a range reading there), possibly moving the pan/tilt head, and allowing for the target point to be specified in a number of coordinate systems. Beyond this, the software must combine these functions to calibrate the instrument. In addition, the software allows for easy access to frequently used combinations of these basic functions. Also, a number of control functions allowing direct communication between the user and the electronics are provided. Finally, status and error indication flags are provided.

Operational use of the functions described below is detailed in Appendix C, and the summaries given here are keyed to that appendix.

The control functions include an azimuth slew (move instrument to specified azimuth, take and return a range reading), an elevation slew, an azimuth scan (move instrument from present position to new azimuth, taking readings at each point along the way, and, if requested, use DMA input), an elevation scan, an azimuth reset, and an elevation reset. The resets not only move the instrument to its zero position (α = 730 for azimuth reset, ε = 738 for elevation reset), but in addition clear the device after "skip-step" errors so that accurate beam pointing readings (α, ε) can be assured. Other control functions permit the electronics to be reset (cleared and initialized) and various tests (scan busy, power on, data ready) to be performed.

Several functions are made easily available to the user. The simplest of these is the beam reset function, which resets both azimuth and elevation. A second function slews the laser to the specified laser step (α, ε) and takes n range readings. The average range number $\bar{r}$ is returned. If $n > 1$, then the variance of the readings is also returned.

The third set of functions reads the pan-tilt head or moves it to a specified (ϕ, θ). Each time the pan-tilt head is moved, the matrix T_A^R is recalculated and saved for future use. The pan-tilt line of sight vector, expressed in ARM coordinates, is returned to the user or calling program whenever the pan-tilt is read or moved.

The fourth function provided is the (re)calibration procedure. Here, the pan-tilt head is moved to a prespecified location, and 50 range readings are taken at each of two calibration points. One calibration point is atop the arm, the single stationary point in the middle of the top of the support post, 99.82 cm from the mirror. The second calibration point is at the back of the electronics rack (Fig. 3-1), 245.87 cm from the mirror. The averages of the 50 range readings at each calibration point are compared with the known distances to these points to yield the constants of the assumed linear relationship between range r' and range reading $\bar{r}$. Then the pan-tilt assembly is restored to its precalibration position and the laser is reset, ready for use.

An initializing command to the LRF software sets an automatic recalibration time interval. Thermal drift necessitates periodic recalibration. The automatic (i.e., time-dependent) recalibrating can be suppressed in order that recalibration only be done when specifically requested.

The fifth function performed by the LRF software is coordinate transformation. A vector in any of the frames LST, RPT, or ARM can be re-expressed in any other of these three frames.

The sixth function is the scanning of a line. The line endpoints can be expressed in any of the three coordinate frames ARM, RPT, or LST, and the repointing of the pan-tilt assembly to the center of the line can be requested as an option as well. The LST (α, ε) and associated ARM (X, Y, Z) are returned for each scanned point. The scanning procedure generates a sequence of lattice points (Recall that (α, ε) are restricted to the integers, as stepper motors are used to drive the laser) which most closely follows the desired line.

The final function made available as an integral part of the software package is the "stop" function, which terminates the program after closing the mirror completely. The mirror is closed to avoid dust and scratches when the apparatus is not in actual use.

The software performing these functions, as all the laser software, is coded in Fortran and assembly language on the General Automation SPC 16-85. The basic software package described above runs in less than 6K of core. This software is made available as a subroutine (LRF) to other users, and also has been combined with two supplemental functions and a teletype driver for stand-alone use.

The supplemental functions are a rectangle scan and a vehicle obstacle scan. The rectangle scan works like the line scan, accepting four corners expressed in any of the three coordinate frames. Up to 20 parallel lines spanning the rectangle are scanned and the highest (maximum Z in arm coordinates) point is saved. It is assumed that the highest point is part of a rock, and the area about that point is (re-)scanned to determine the rock's orientation. The rock's position and orientation are then output to a file. This rectangle scan can easily be combined with the manipulator software to yield an end-to-end demonstration of integrated laser-manipulator operation.

The second supplemental function provided with the teletype driver is an obstacle scan at 3 meters in front of the vehicle. Here the beam is swept side to side in an effort to locate severe adjacent-point range differences. If one is located, a single bit is returned to the vehicle drive software.

All calls to the laser software result in an error/status flag being returned to the caller (or teletype). This flag reports violations of laser azimuth or elevation limits, laser drive step-skipping (which would result in the beam position (α, ε) being unknown), range numbers (r) out of the domain of possibility (either because the power supply is off or because no signal is returned), pan-tilt errors, and warnings that conversions to LST coordinates are out of the acceptable domain of operation.

A user's guide file to the LRF software and program flowcharts are provided in Appendices C and D.

V. APPLICATIONS

The LRF software has only relatively recently been made operational and available to the Robot Research Program as a package. Nevertheless, the LRF instrument and software have already been applied to several tasks, with more currently being investigated. In this section, these applications are described.

A. Rockfinding

The rectangle scan described in Section IV as the first supplemental function has been combined with the manipulator software to yield automatic scanning, recognition, position and orientation determination, and retrieval of the tallest rock in a 30 cm x 71 cm scanned region. The elevation of the scanned points is displayed as intensity data on a video monitor (Figs. 5-1, 5-2). Higher points appear darker on the displayed image. The range data is converted to ARM coordinates, the Z coordinate of which is converted to an integer corresponding to an intensity datum on the monitor.

Errors in the end to end sequence include all laser and pan-tilt pointing errors, laser ranging errors, surface reflectance and gray level contributions, vehicle sag and other transformation errors, and arm positioning and calibration errors. In essentially all cases, the laser instrument and algorithm precision are sufficient for the rock to be recognized and located by a laser beam aimed at it, but only in about half the cases to date are the position and orientation data, transformations, and arm positioning and calibration accurate enough to result in the target rock being successfully retrieved and deposited in a sample box. Continuing work on the use of arm-mounted proximity sensors as grasping aids (Ref. 24) is expected to result in a much higher success rate.

B. Vehicle Obstacle Scan

The side-to-side laser scan described in Section IV as the second supplemental function is to be used as an in-motion early warning obstacle detector for vehicle motion. The beam is swept along a line 3 meters in front of the vehicle at ground level, roughly from the outside of one wheel to the outside of the other, back and forth. No coordinate transforming of the raw data is

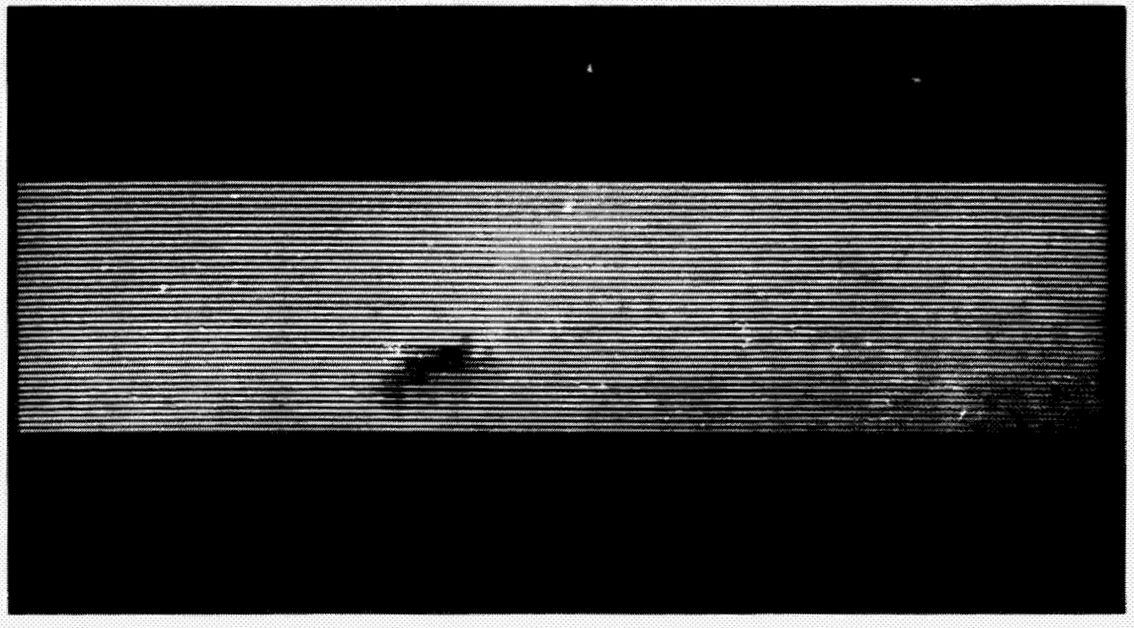

Figure 5-1. LRF-Generated Elevation Picture of Rock

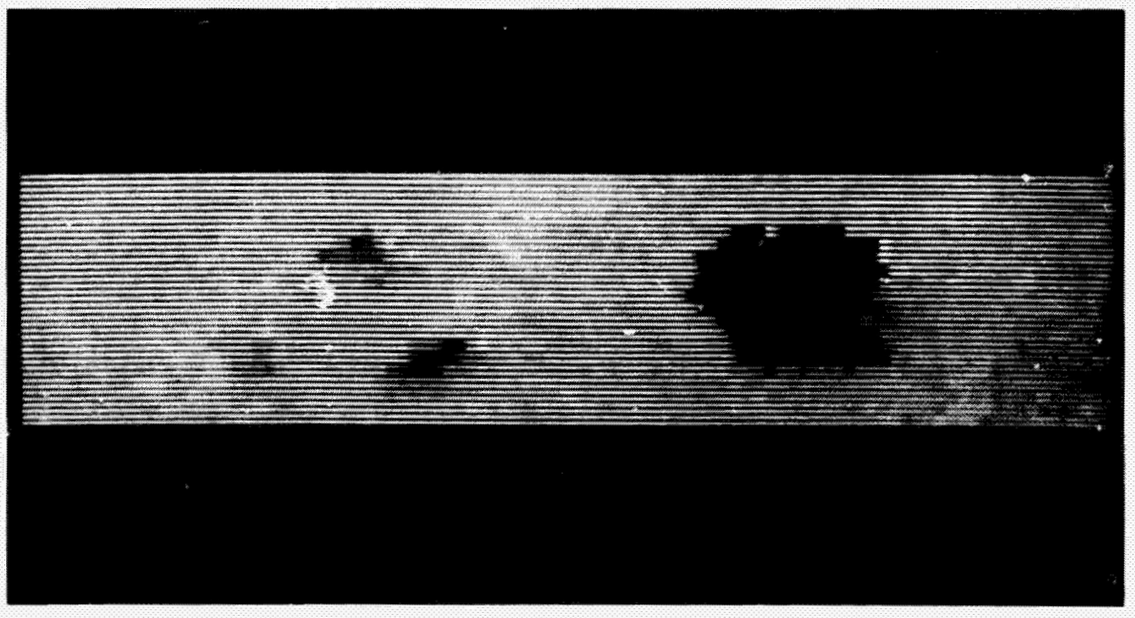

Figure 5-2. LRF-Generated Elevation Picture of Three Rocks and a Block

performed, but rather, sharp differences in the raw range data themselves are look d for. Figure 5-3 graphically illustrates the returned range data when no obstacle is present and when an 8 cm high box is present. The criterion for an obstacle currently being used is a range number difference of 10 or greater between successive points. This corresponds to an actual range difference of approximately 7.84 cm. If this criterion is met, a flag is returned to the vehicle drive program, which can then stop the vehicle, gather more data about the obstacle and surrounding environment, and plan a new path.

The present vehicle is heavy relative to the available power to drive it, so that even an 8 cm object is an obstacle. Range differences do not correspond directly to differences in elevation, and it is conceivable that an obstacle with smooth edges and no real corners could remain undetected. The described scan algorithm and obstacle criterion thus represent a compromise between simplicity (and speed) of operation, on the one hand, and effectiveness on the other.

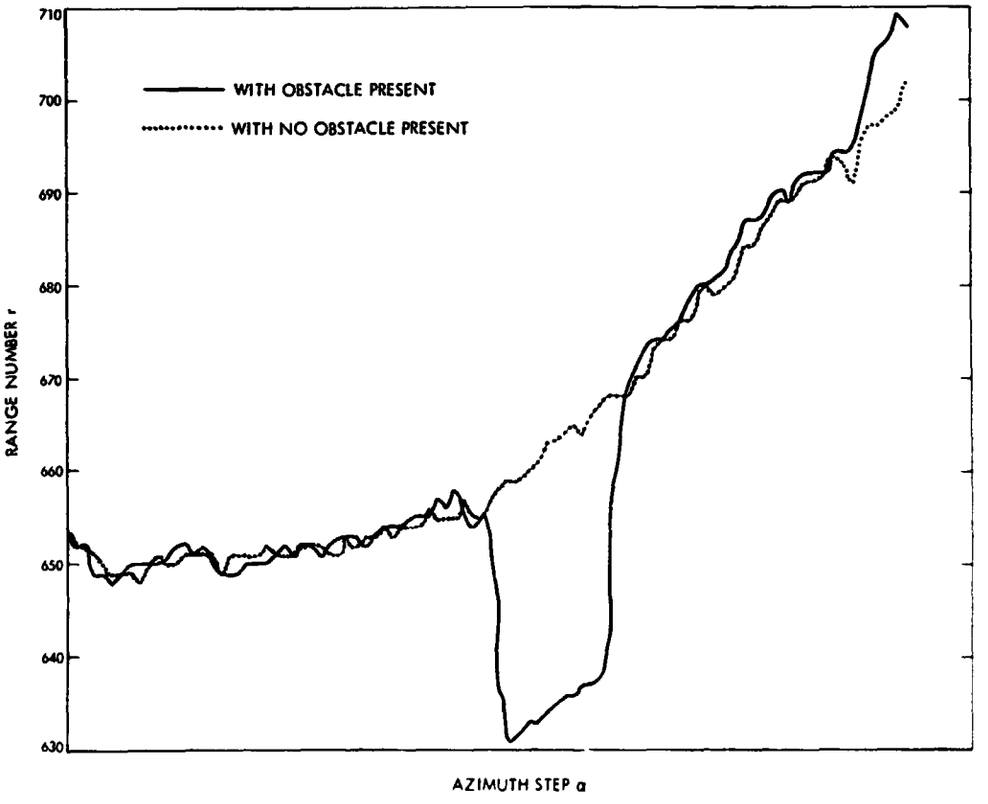

Figure 5-3. Vehicle Obstacle Scan LRF Data

Another factor to be noted that tends to diminish the thoroughness of the scan is the effect of vehicle motion. A scan takes about 2 seconds (94 points at 50 points/second). By moving the vehicle slowly in areas of more danger or less complete knowledge of the environment, and by comparing detected obstacles with objects already known (see below), the laser in-motion obstacle scan is expected to be a useful adjunct to the robot's safety system.

C. Obstacle Mapping

The first user application to which the laser system has been put is obstacle mapping. Before the vehicle is moved, a terrain map of the area must be obtained. A single television image could be used for this purpose, but then the information obtained is only two-dimensional; its location along the line of sight would remain unknown. Television images from two cameras or from the same camera at two locations could provide three-dimensional data, but only at the expense of correlating the video data from the two images. Accordingly, the LRF, which provides three-dimensional data from a single "image," has been used to map the terrain in the vicinity of the vehicle. Figure 5-4 shows a processed terrain map of a 3 meter square in front of the vehicle. "Safe"

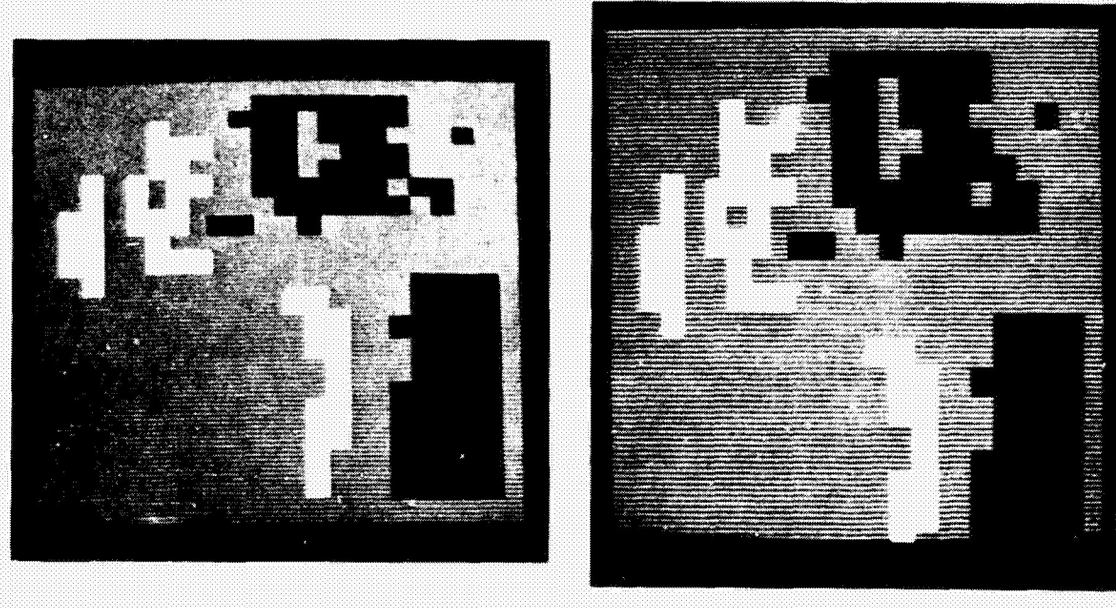

Figure 5-4. Obstacle Map

(i.e., obstacle-free) regions are shown in gray, unsafe ones (those whose elevation is 15.24 cm or more from the floor, as defined by the vehicle wheelbase) in white, and unknown regions in the shadow of obstacles in black. The right obstacle map in Fig. 5-4 shows a processed version of the left map in which adjacent obstacles have been merged. A series of terrain maps covering the area between vehicle and target is made, and then the terrain can be searched for a safe path.

D. Range Pictures

The LRF is quite sensitive to changes in range. A demonstration of its sensitivity and ability to yield data of sufficient quality for scene analysis work is presented in Figs. 5-5 and 5-6. These figures are "rangepics." Range data (integers from 0 to 1023) have been converted to intensity data (0 to 255) and displayed on a video monitor. The pictured features are approximately 2 to 3 m in front of the vehicle. The laser data were taken over a complete lattice of 64 x 64 LRF azimuths and elevations. As displayed, no correction for angular distortion has been made. The box-like structures in the images

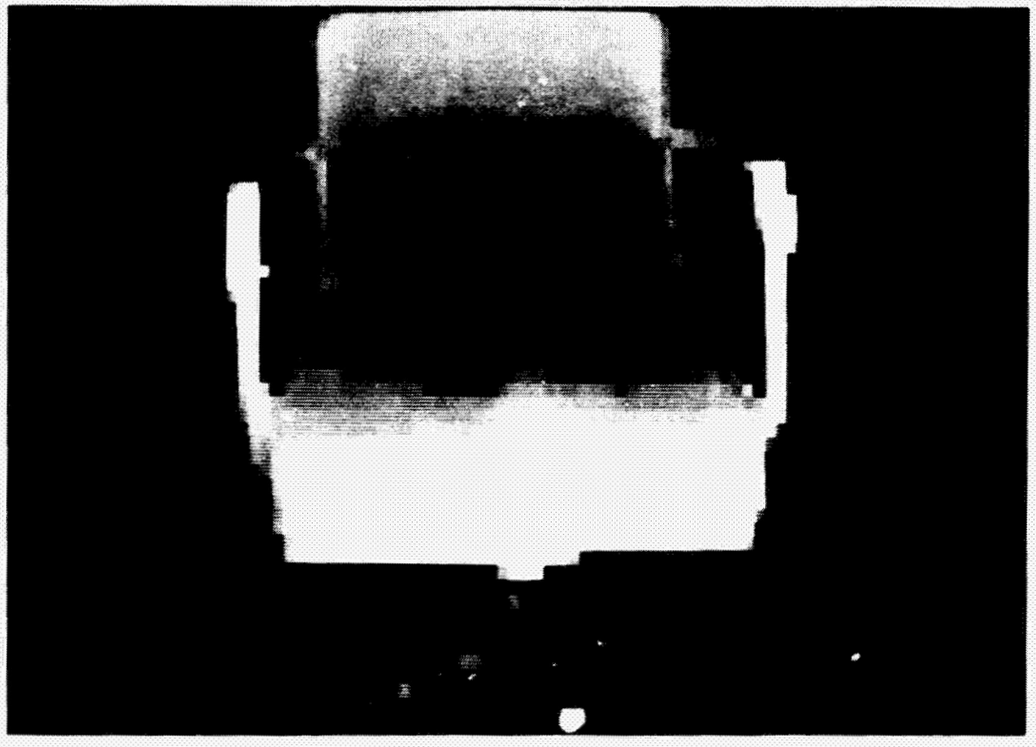

Figure 5-5. Range Pictures

Figure 5-6. Rangepic

result from the fact that each laser datum is displayed as a 4 x 4 array of monitor pixels in order to fill the screen.

E. Picture Segmentation and Scene Analysis

The application of scene analysis software designed for video data to LRF data is currently being investigated. The straightforward segmentation of laser rangepics is one approach being considered. Aiming the LRF at specified video image points for range data or dual camera image-matching, tracking of the laser beam as it moves through a visual scene, and using the laser to confirm the existence of edges and object boundaries are other avenues being considered. It is anticipated that the dual TV/LRF system will ultimately provide the JPL robot with a powerful perceptive apparatus.

VI. SUMMARY

A scanning laser rangefinder for a robotic vehicle has been described. Its ranging accuracy approaches 2 cm with optimum adjustment of the constant-fraction discriminator. The dominant error source is the effect of unknown reflectivity and angle of incidence of the target surface. Pointing accuracy of the instrument itself is well within 0.1 deg, a small error compared to the range error. However, the cumulative effects or errors induced by mounting the LRF on a pan-tilt assembly, putting the entire apparatus on a vehicle, and then relating the results to the environment also tend to degrade the performance of the LRF.

We feel that the instrument could be significantly improved with further development effort. First, current semiconductor techniques appear capable of reducing the risetime of the light pulse significantly, and since the accuracy at present is directly dependent on risetime, this would be a practical benefit (Ref. 34). Improvement may result even though the peak pulse power may decrease, if pulse repetition rate and risetime can both be improved.

A second approach, independent of the light pulse shape, involves improvement of the timing decision through more effective fast pulse electronics. Such improvement could be obtained by performing a measurement of the reflected pulse height and using the information to correct measured range. A conventional intensity image as seen under illumination by the laser source could be obtained as a by-product.

Alternatively, better schemes for timing independently of intensity could be sought, either in terms of improved constant-fraction discrimination, or by means of multiple data points from each pulse (Ref. 25), the ultimate being a real-time cross correlation.

The LRF is not at present driven by any requirement for a high data rate, and indeed, its data rate is very low. Efforts to increase the data rate will encounter a limitation due to basic noise in the detected signal at about 100 data points per second, with the present laser power. Higher data rate

will involve a tradeoff in which uncertainty of a single point increases proportionately to the square root of data rate.

Even as the system stands today, numerous practical applications have already been made and more continue to be investigated. The results of these investigations will be reported as the continuing integration of the LRF and its software with vehicle and vision systems progresses.

VII. REFERENCES AND NOTES

1. Berdahl, M., and Harrison, R. G., Fast Rise Time, High Pulse Repetition Rate Pulser for Solid State Laser, New Technology Report NTR 3014/NPO 13455, Jet Propulsion Laboratory, Pasadena, California, Nov. 1973 (JPL internal document).

2. Whitney, W. M., "Human vs. Autonomous Control of Planetary Roving Vehicles," IEEE Symposium on Systems, Man and Cybernetics, Dallas, Texas, Oct. 1974, Institute of Electrical and Electronics Engineers.

3. Payne, J. M., "An Optical Distance Measuring Instrument," Rev. Sci. Instr., Vol. 44, p. 304, 1973.

4. Froome, K. D., and Bradsell, R. H., J. Sci. Instr., Vol. 43, p. 129, 1966.

5. Woodbury, E. J., "Some Aspects of Laser System Design," Ann. N.Y. Acad. Sci., Vol. 122, p. 661, 1965.

6. Proceedings, Symposium of Laser Range Instrumentation, El Paso, Texas, Oct. 1967, Society of Photo-Optical Instrumentation Engineers.

7. For example, Hewlett Packard 3800A, Distance Meter, or AGA Model 76, Geodimeter.

8. Spectra Physics Model 3A Geodolite.

9. Meyers, F. J., "Application of Pulsed Lasers to Range Determination," Transactions IRIS Meeting, San Francisco, California, Apr. 1971, Infrared Information Symposium.

10. Austin, M. E., et al., GaAs Laser Radar Components and Techniques, TR 407, Final Report, Contract NAS 9-105, Lincoln Laboratory, Massachusetts Institute of Technology, Oct. 1965.

11. "Optical Ranging," NASA Literature Search No. 12087, June 1970, and DDC Report Bibliography No. 03960 (untitled), 1970, both unpublished literature searches prepared for A. R. Johnston, Jet Propulsion Laboratory, Pasadena, California.

12. Walters, E. B., Laser Range-Tracker, MSC-10277, Lyndon B. Johnson Space Center, National Aeronautics and Space Administration, Nov. 12, 1969.

13. Final Report for Laser Tracking and Ranging System, RCA Astro Electronics Division, Princeton, New Jersey, 1969.

14. Kelley, R. C., and Reynolds, R. D., A Laser Rangefinder, MSC-00177, Lyndon B. Johnson Space Center, National Aeronautics and Space Administration, Aug. 1969.

15. Shumate, M. S., in 3-D Multilateration; A Precision Geodetic Measurement System, TM 33-605, Jet Propulsion Laboratory, Pasadena, California, Mar. 15, 1973.

16. Development of Multimode Remote Manipulator Systems, Annual Report No. 2, C-3901, Draper Laboratory, Massachusetts Institute of Technology, Jan. 1973.

17. Brain, T., "The Scanning Laser Rangefinder," in Artificial Intelligence Research and Applications, SRI Progress Report, Apr. 1973 to Apr. 1974, ARPA Contract No. DAH C04-72-C-0008, N. Nilsson, Ed., Stanford Research Institute, California.

18. Herzog, D. G., "Precision Hover Sensor for Heavy Lift Helicopter," RCA Engineer, Vol. 18, No. 2, Aug.-Sept. 1972.

19. Reisse, R., Cheley, R., and Poultney, S. K., "Single Photon Detection and Subnanosecond Timing Resolution With the RCA 31034 Photomultiplier," Rev. Sci. Instr., Vol. 44, p. 1666, 1973.

20. Model 447, Time to Pulse Height Converter, Ortec Corp., Oak Ridge, Tennessee.

21. For example, Half-max Discriminator, Nanofast Corp.. Chicago, Illinois.

22. Dobrotin, B. M., and Scheinman, V. D., "Design of a Computer Controlled Manipulator for Robot Research," Proceedings, Third International Joint Council on Artificial Intelligence, Stanford University, Calif , Aug. 20-23, 1973.

23. Johnston, A. R., Optical Proximity Sensors for Manipulators, TM 33-612, Jet Propulsion Laboratory, Pasadena, California, May 1, 1973.

24. Johnston, A. R., An Experiment in Manipulator Control With Proximity Sensors, TM 33-678, Jet Propulsion Laboratory, Pasadena, California, Apr. 1, 1974.

25. Miyake, K., Appl. Opt., Vol. 15, p. 1684, 1976.

26. MPC Products Corp., Chicago, Illinois.

27. Balzer No. B-IR-844-14.

28. Eccosorb.

29. Kawamoto, H., and Miller, D. J., "Nanosecond Pulsing of GaAlAs Lasers With Carrier Injection Triggered Trapatt Devices," Technical Digest, Optical Fiber Transmission, Optical Society of America, Jan. 7-9, 1975.

30. Unitrode Type GA 201A.

31. Gedcke, D. A., and McDonald, W. J., "Design of the Constant Fraction of Pulse Height Trigger for Optimum Time Resolution," Nucl. Instr. Methods, Vol. 58, p. 253, 1968.

32. Constant Fraction Discriminator, Model 1427, Camberra Electronics, Meriden, Conn.

33. Cardone, L., et al., Final Report for Lunar Roving Vehicle Hazard Detection, Contract NAS 8-25109, George C. Marshall Space Flight Center, National Aeronautics and Space Administration, May 1970.

34. Ghigo, F. D., Shelus, P. J., Silverberg, E. C., and Faller, J. E., "Laser Range Measurements Using Non-Gaussian Pulse Shapes," Appl. Opt., Vol. 15, p. 2621, 1976.

APPENDIX A

SUMMARY OF LASER RANGEFINDER SPECIFICATIONS

Table A-1. Specification Summary

	Laboratory	Contact	Model No.	Cost	Product Avail?	Application	Configuration				Scan	R_{min}	R_{max}	ΔR at R	Data Rate Sec^{-1}	Size (cm)	Power	Re out
							Laser	λ	Mode	Coop Targ?								
1.	AGA	Robert Landis	76	4.1	yes	Surveying	--	--	--	yes	no	few meters	2 km	±1 cm 25 m	--	30 × 25 × 20	battery	Digital display
2.	Hewlett Packard	--	3800 A	4.0K	yes	Surveying	--	IR	--	yes	no	--	2 km	±1/2 cm	slow	32.5 × 25 × 12.5 17.5 × 17.5 × 22.5	12 W battery	Manual nulling
3.	Spectra-Physics	--	3A	50K	yes	Aircraft map	HeNe	6328	CW	no	no	<3 m	3 km	3 cm	10^3	82.5 × 32.5 × 37.5	4 0 W	Analog
4.	Hughes	Knapp	Many 35 models	--	no off shelf	Military	GaAs	--	pulse	no	--	--	--	--	--	--	--	--
							NdYag	1.06μ	Q/SW	no	--	--	--	--	--	--	--	--
5.	Int'l Laser Sys.	W.C. Schwartz	LWR 100	--	yes?	--	NdYag	1.06μ	Q/SW	no	no	200 m	10 km	5 m	10	15 × 15 × 65	--	D or A
6.	ITT-SF	T.Flom	--	200K	no	NASA MSFC	GaAs	0.9μ	pulse	no	yes	--	30 m	30 cm	$< \times 10^3$	20 × 20 × 45 15 × 15 × 45	~27 W	?
7.	RCA	P. Sealy	--	40K	no	Military	GaAlAs	0.84μ	pulse	no	yes	--	30 m	30 cm	10^3	--	--	D
			Metric camera	--	no	NASA MSC	Ruby	0.69	Q/SW	no	--	--	200 km	--	1/15	30 × 30 × 30 approx.	50 W	
8.	JPL	M. Shumate	Breadboard	--	no	Geodetic	GaAlAs	0.84μ	pulse	yes	no	~10 m	?	±3 cm	$1-10^4$	--	110 V	D
9.	MIT Draper Lab	Watson	Breadboard	--	no	Telerobot	Led	--	CW 50 MHz	yes	no	--	3 m	1 mm	--	--	--	Digital display
10.	MSC	D. Lilly	Breadboard	--	no	Aircraft	GaAs	0.9μ	pulse	no	no	<10 m	50 m	10 cm	10^3	--	--	D
11.	Zenick Assoc.	R. Zenick	LRF250X	12K	no	Military	GaAs	0.9μ	pulse	no	no	--	10 km	1%	10^3	15 × 15 × 40	115 Vac	A or D
12.	SU AI Lab	T. Binford	--	--	no	Telerobot	Laser/TV				no	~1 m	~1 m	1 mm	1.5×10^4	--	--	Computer Interface
13.	SRI	J. Munson	--	--	no	Telerobot	Triangulation Sensor				no	~1 m	~10 m	5 cm	~10 (?)	--	--	D

APPENDIX B
LRF DESIGN AND PERFORMANCE

B-1. Optical Head

The rangefinder optical head, illustrated in Fig. 2-1, consists of three modules. The upper module is a modified Surveyor TV camera mirror unit, originally a part of a TV system designed for a Surveyor spacecraft; the middle module consists of the laser, laser pulser and the necessary optics for collimating, transmitting and collecting the laser radiation; the lower module houses the photomultiplier detector. The overall size of the optical head is 20 cm. wide, 15 cm. deep, and 60 cm. high.

The Surveyor gimballed mirror unit was modified to meet the requirements of the LRF. To obtain the desired 5 milliradian stepping increment for the LRF required that the original stepper motors be replaced. Size 11 permanent magnet stepping motors with integral gear heads were selected (Ref. 26). The complete unit was smaller than the motor it replaced. The mirror stepping rate is presently 50 steps per second, but the rate could be increased to perhaps 300 steps per second with appropriate redesign. The limits of scan are 350° in azimuth and 50° above and below the horizontal in elevation. The lower scan limit in elevation is a result of the lower part of the instrument physically blocking the view.

The original azimuth bearing was replaced by a free ball type bearing with machined-in-place races. The modified bearing has a clear inside diameter of three inches to accommodate the optics, yet did not require extensive rebuilding of the housing.

Figure B-1 shows a more detailed cross section of the second module containing the optics. The laser pulser is enclosed in a can which is electrically isolated from the outer case. It is mounted to a heavy bracket which serves as a heat sink for the laser, and a portion of the can is made removable to permit access for repairs or adjustments. The laser is an RCA No. C30012 injection laser diode with a light-emitting area of 0.02 x 0.15mm, and a peak power output of 3 watts, emitted into a half angle of approximately 15°.

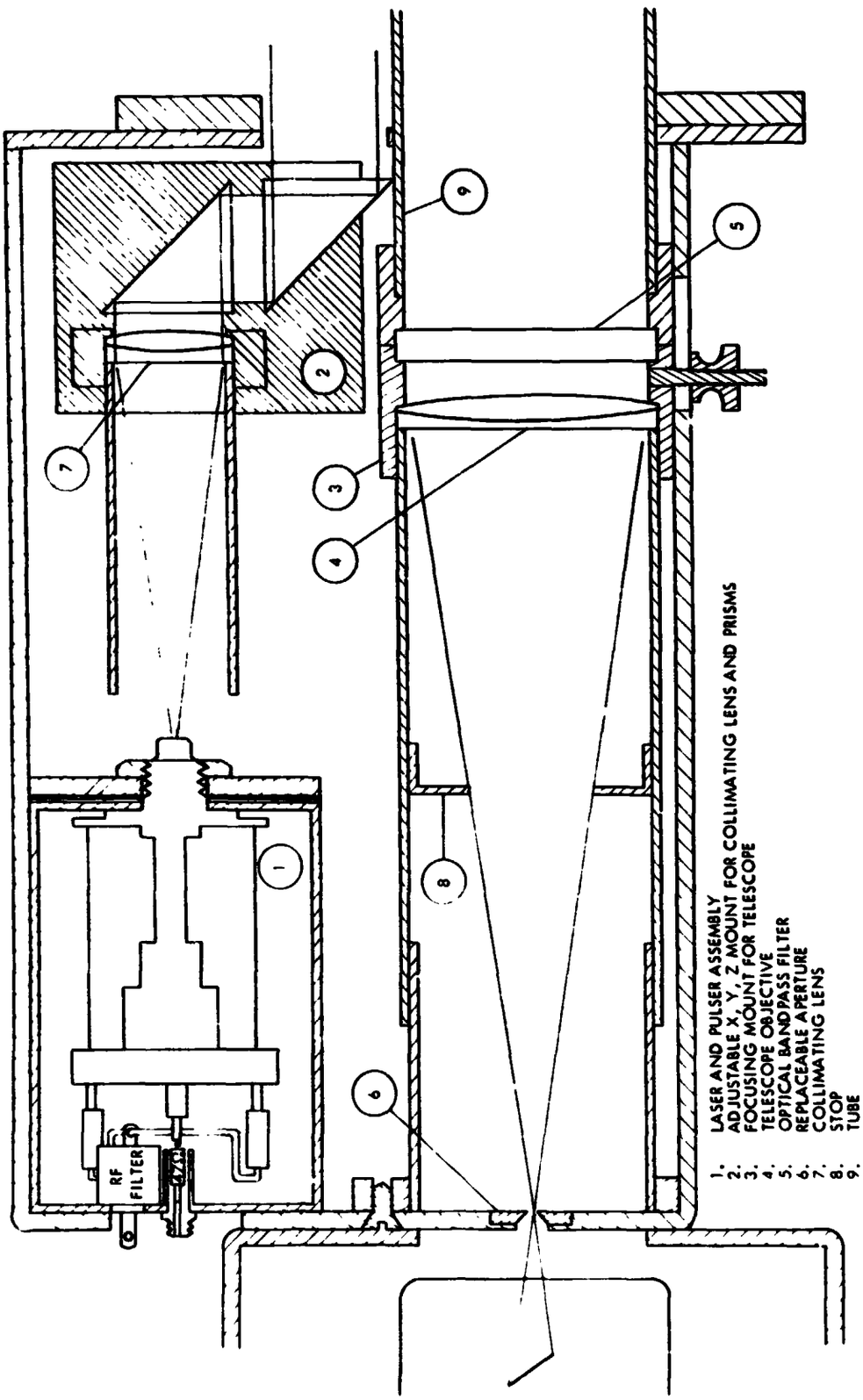

Figure B-1. LRF Optics Module Containing Laser Pulser and Telescope

The one in current use has a wavelength of 844 nanometers, and its spectral width $\Delta\lambda$ between 50% intensity points is 3.5 nanometers. Substitution of RCA No. C30013, a similar but higher power laser, could be made to obtain a higher power level at the target, but a proportionately larger spot would be produced. The collimating lens is 25 mm in diameter and 7[illegible] mm in focal length, producing a line image whose angular length is 2 milliradians. After collimation, the light passes through two right angle prisms which direct it through the azimuth bearing to the mirror. The collimating lens and prisms are mounted to a fixture which permits adjustment in each of 3 mutually perpendicular directions. This is necessary in order to focus the laser image on the target and place it laterally where it will be seen by the collecting telescope.

Light returning from the scene is passed through an optical filter having 40% transmission at 844 nanometers and a bandwidth (FWHM) of 14 nanometers to reject ambient light (Ref. 27). Laser and filter must be individually matched, as the laser wavelength can vary between samples. A field-of-view aperture at the focal point of the collecting telescope further reduces the ambient light level. This aperture is removable, and the one in use has an opening 0.5 x 0.28mm, oriented to line up with the return image. Care must be taken to avoid scattered light from the laser entering the photomultiplier.

The lower module of the rangefinder is shown in further detail in Fig. B-2. The photomultiplier is an RCA No. C31034, a 5 cm dia., head on, 11 stage photomultiplier having a gallium arsenide photocathode with a projected area normal to the returning beam of 4 x 10mm. The spectral response of the C31034 extends from 200 to 930 nanometers with the peak at 830 nanometers. Nominal anode sensitivity at the peak is 4.1×10^4 amps per watt with a D.C. supply voltage of 1500 V. The tube is oriented to align the long dimension of the photocathode with both the laser image and the relative motion of the image due to parallax. Surrounding the photomultiplier is a magnetic shield which is electrically tied to the cathode. The remaining space is filled by a carbon loaded spongy material (Ref. 28) to help reduce electromagnetic ringing and noise. The distance from aperture to photocathode is 3.4 cm. A field lens immediately following the field stop of the telescope is helpful to avoid movement of the light spot on the cathode as range varies.

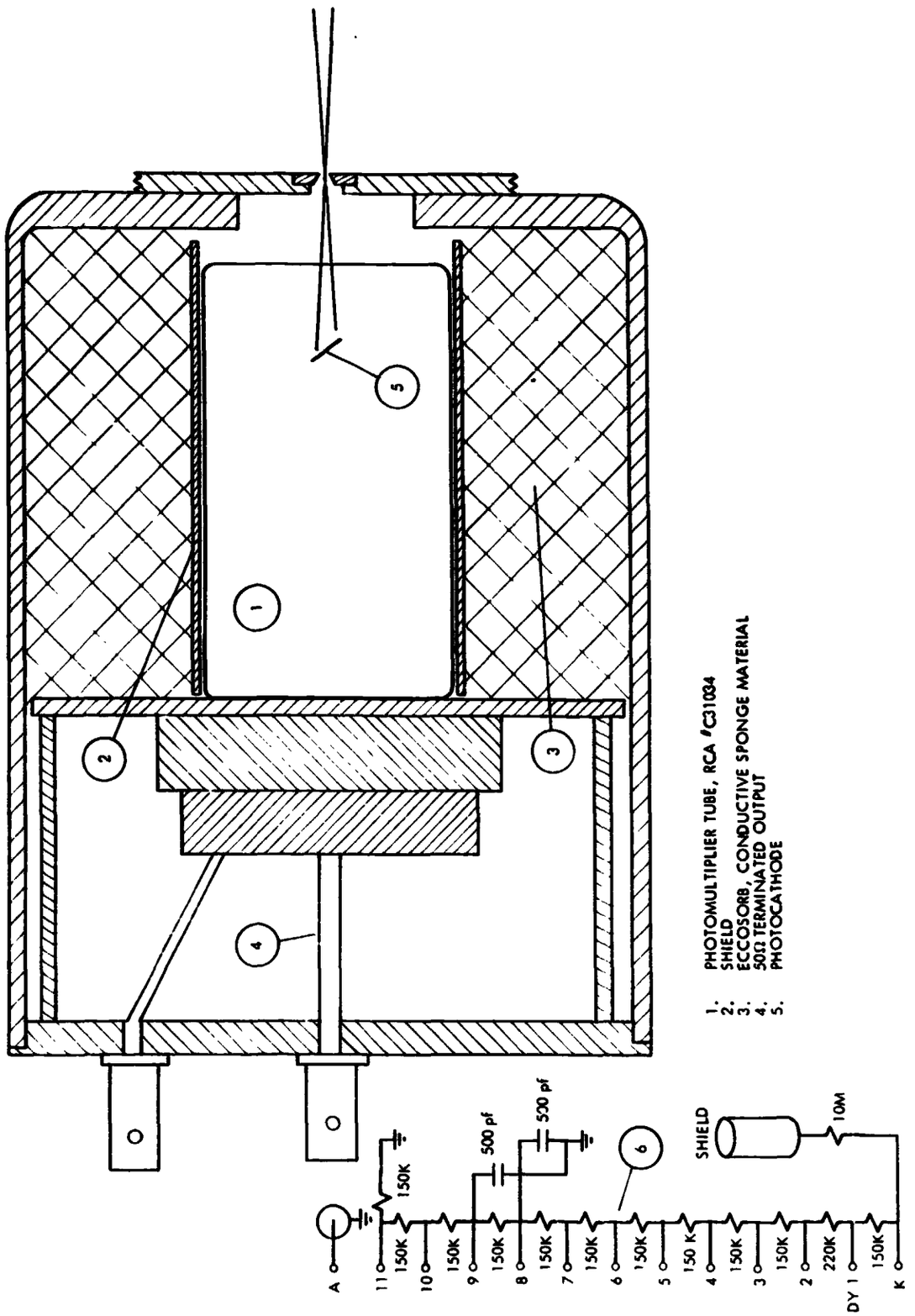

Figure B-2. Lower Module Containing Photomultiplier

The photomultiplier anode drives a 50 ohm terminated coax line directly, with great care being taken to minimize lead length outside of the transmission line. The circuit shown in the inset of Fig. B-2 supplies voltages for the dynodes.

The following quantities related to the LRF optics were determined:

1.	Peak output power, P_{pk}, of laser image	0.22 watts
2.	Transmission of lens	0.8
3.	Transmission of filter (measured)	0.36
4.	Solid angle subtended by telescope objective from target	10^{-4} steradian
5.	P_{pk} to photomultiplier	6.3×10^{-6} watts
6.	Sensitivity of photomultiplier (measured) at 844 nanometers	5.1×10^{3} amps/watt
7.	Calculated peak output voltage, V_{pk}	1.6 V
8.	Measured photomultiplier peak output voltage	0.16 V

The difference between the calculated and observed outputs is felt to be due to the photomultiplier responsivity being lower than nominal.

B-2. Laser Pulser

A light pulse with the minimum possible rise time and maximum intensity is needed, and the resulting requirements for both fast rise time and high current from the pulser are conflicting. Conventional transistor pulse circuits were found inadequate. Avalanche transistors in transmission line configuration can yield a fast rise time, but low current. We selected a silicon SCR (Thyristor) circuit to dump energy from a group of capacitors which were arranged in a coaxial configuration for low inductance (Ref. 1).

Since our pulser was designed, other approaches have been described that may be of interest (Ref. 29) because they may be able to produce a faster rise time.

A study of commercially available pulsers and pulse circuits indicates the pulse rise time and peak current are limited by the avalanche characteristic of the switching element, in this case the thyristor. Also, when pushing toward short pulses, the turn-on and recovery time of the inverse current protection diode become important factors.

A simple capacitor discharge through a gate driven thyristor circuit was chosen. A combination of several parallel thyristors was used in order to obtain high peak current together with good rise time.

Capacitor lead length will affect the total circuit inductance, so in order to minimize this inductance, a circuit configuration in the form of a cylinder was adopted, with the capacitor current passing down the axis of the cylinder, splitting radially and returning distributed among many leads arranged in the form of a concentric cylinder, as shown in Figure B-3. The separate capacitor discharge currents are collected through a header, down the axis of the cylinder through the semiconductor switching devices, and directed to the laser diode supported in a common ground header at the opposite end of the cylinder.

CORNING glass dielectric type capacitors were used. This type was selected not only because of its convenient size and shape, but because internally it appears to have many physically short, interleaved plates, providing a short path for draining the charge.

Assuming that synchronous triggering can be obtained, the peak current obtainable is limited only by the number of switching devices which are placed in parallel. It is apparent from the literature provided by the manufacturers of switching thyristors that rise time increases in proportion to peak current switched, and that rise times of less than 10 nanoseconds push the state of the art.

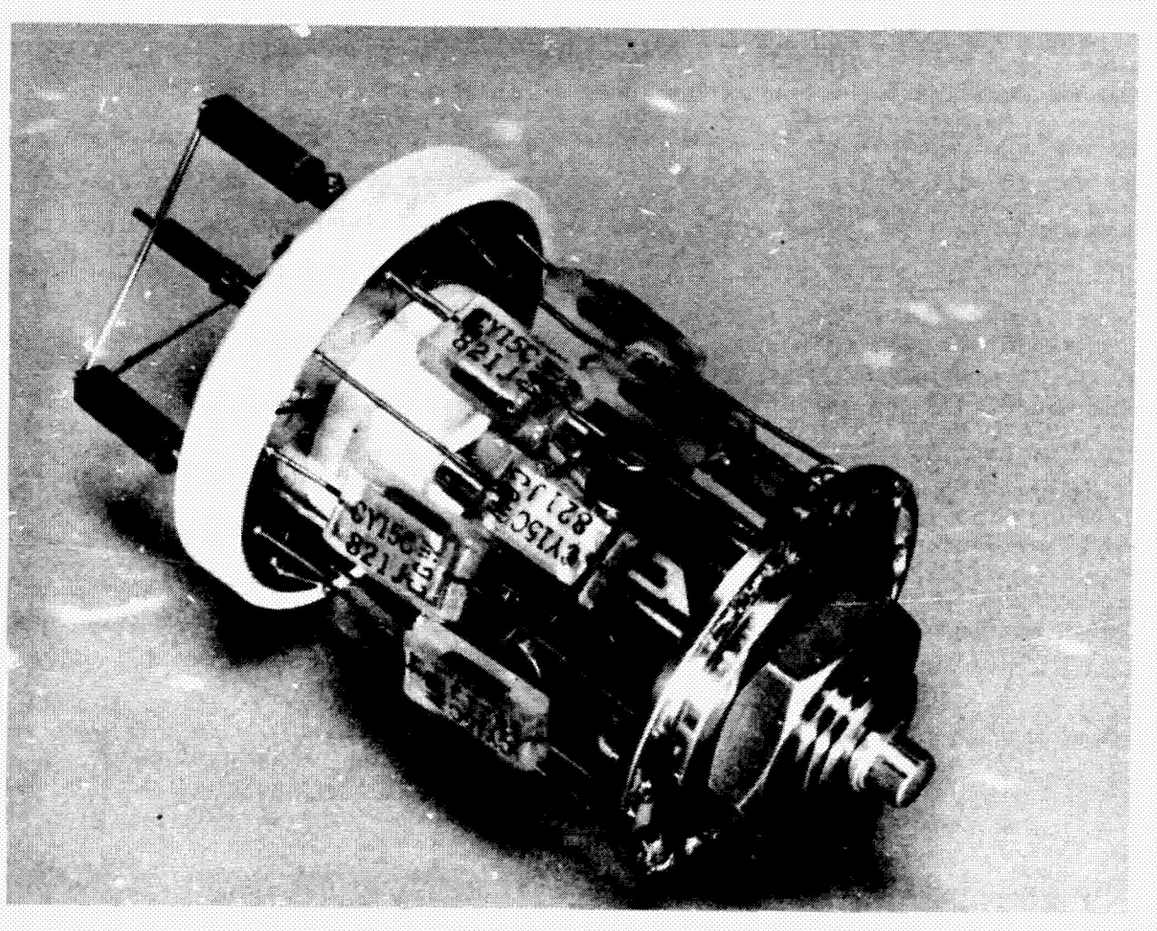

Figure B-3. Photo of Laser Pulser

It appeared that the desired rise time might be obtained by using a parallel combination of three thyristors (Ref. 30) which are rated at 20 nanoseconds rise time for switching 30 amperes peak, but operating them at a lower peak current.

Circuits of this type often use a small series resistor for monitoring pulse current and to supply damping to control ringing. This resistor was omitted in order to obtain the fastest possible rise time. Instead, reverse direction diodes were installed across the laser in order to provide damping and to limit the amplitude of any reverse voltage which might appear across the laser. It was found that twelve diodes in parallel across the laser reduced ringing amplitude to a tolerable value. The diodes used in the final version are HP 5082-1006 Schottky units, but IN4007 fast turnon, high current diodes were also found to be suitable.

The circuit of the pulser is shown in Figure B-4. Three banks, each consisting of four parallel 820 pf capacitors, constitute the 0.01 mfd charge storage capacitor. The three banks are resistively charged in parallel from the power supply. Three thyristors having their gates tied in parallel switch the pulse current. Triggering is by a pulse generator which provides a 2 volt positive going square wave having a 10 nanosecond or less rise time. It was decided to

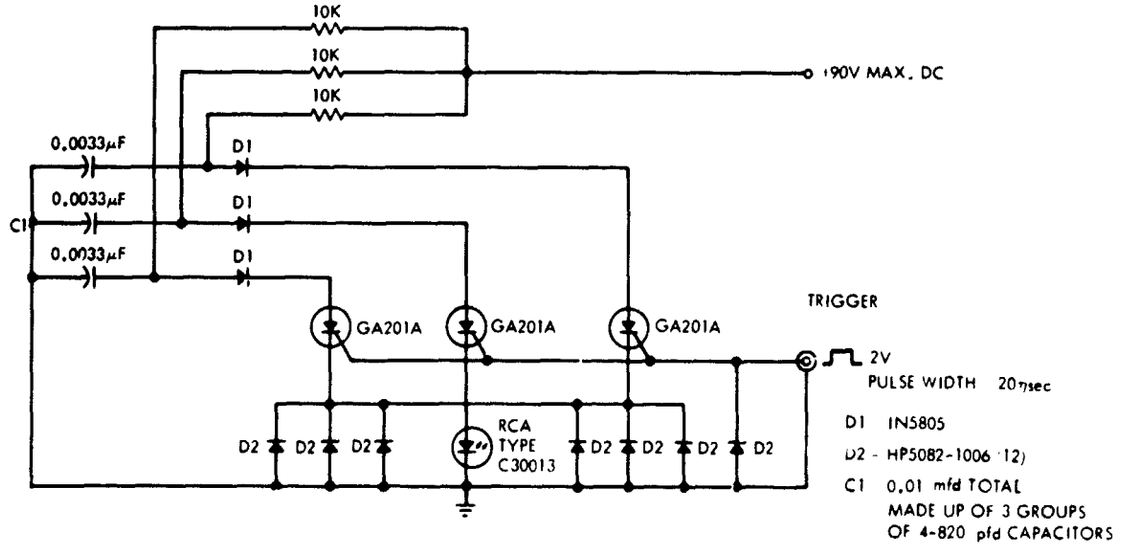

Figure B-4. Pulser Circuit

trigger the thyristor gates in parallel without any special synchronizing circuitry. In order to assure equal sharing of the discharge current, the total circuit capacitance was divided into three groups or banks each having one-third of the total capacitance.

The three series diodes were originally included in the circuit to prevent possible reverse charging of the capacitors and to provide a control point from which a current controlled charge circuit could be operated. However, experience with the circuit suggests they could be eliminated.

The combination of the 10 kilohm resistor and the 0.0033 mfd of each capacitor bank produces a charging time constant of 0.33×10^{-4} seconds, one third of the available change time. The 10 kHz repetition frequency is possible without special power supply circuitry because an inductive undershoot following pulsing permits the thyristors to recover and remain in cutoff (Fig. B-5).

Figure B-6 illustrates some details of the physical design of the pulser. The structure includes two circular brass headers between which the circuit components are installed. One header includes a female threaded portion into which the 8-32 threaded shell of the laser diode is screwed. As the threaded portion of the laser housing is connected to the cathode, the header not only serves a circuit ground but also serves as a heat sink for the laser. The anode lead of the laser fits into a spring loaded clip which is held in place and insulated from the grounded header by a boron nitride or porcelain insert.

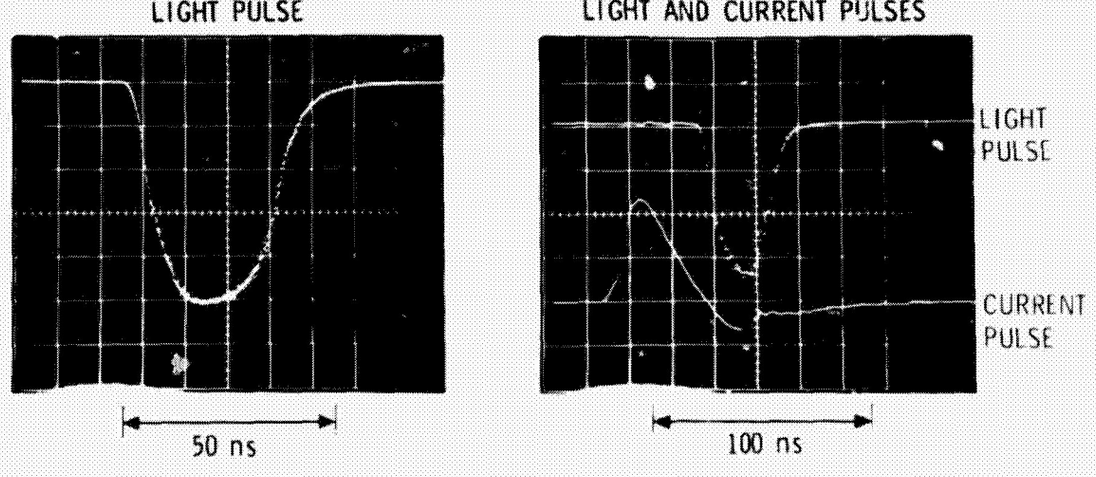

Figure B-5. Pulser Output, Showing Current Pulse and Light Output

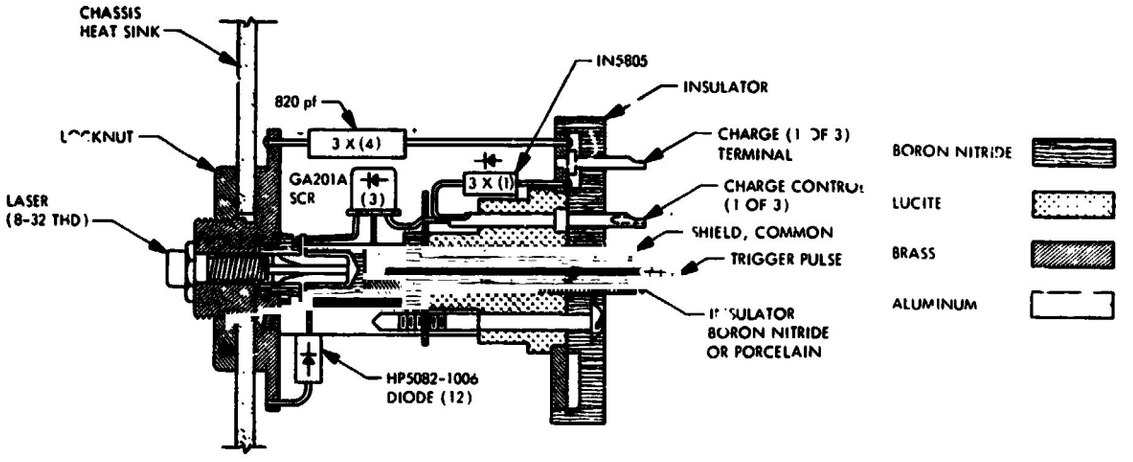

Figure B-6. Sketch of Laser Pulser

The common trigger connection for the thyristors is brought to the gates through the header at the opposite end of the structure by means of a shield tube and concentric Teflon insulator. The gate leads of the thyristors are clipped to correct length and held attached to the trigger electrode by set screws.

The results obtained in testing exceeded expectations by achieving pulses of approximately 30 nanoseconds duration (width at 10% of peak amplitude) with peak currents approaching 100 amperes, at a repetition frequency of 10 kHz. The form of the light pulse is shown in Fig. B-5 as measured by the LRF photomultiplier. We conclude from our testing that the observed rise time of 10 ns is still primarily circuit limited and is not due to either SCR or laser characteristics. Since 10 ns is long compared to the (impulse) rise time of the photomultiplier (~3 ns), the ultimate instrument accuracy is dependent on the laser pulser rise time, and could be improved if the rise time could be shortened.

Note that our estimated peak current is considerably greater than the maximum pulse current specification of the laser, 25A. The large current has not resulted in laser damage because of the short pulse duration. Both the average current and power dissipated by the laser are well within the manufacturer's ratings. Tentatively, we conclude that even larger current pulses would be

tolerated by the laser if they remain sufficiently short. Since timing is done with respect to the rising slope of the light pulse only, the fall time and any associated tail are only detrimental, contributing to device heating.

B-3. Constant Fraction Discriminator

The most critical element in the LRF measurement sequence is the constant fraction discriminator. The theory and design of constant fraction discriminators has been given in the literature (Ref. 31), and our unit was commercially obtained (Ref. 32). Accordingly, we will not discuss the discriminator in any further detail here. It suffices to say that its adjustment is critical if one expects to obtain minimum dependence of measured range on reflected light intensity.

The observed light rise time of 10μs is equivalent to a range increment of 1.5m. Therefore, for one centimeter accuracy, we must measure the arrival time of the reflected pulse within about 1% of the rise time, or put a different way, we must depend on knowing the shape of the leading edge of the return pulse to within 1% in order to make a sufficiently accurate timing decision. Fortunately, our requirement for accuracy is associated with manipulation at ranges of the order of 2m, so reflected light intensity is large and the amplitude of the return pulse can be the maximum tolerable to the photomultiplier, about 1 volt peak into 50Ω. Even so, ringing and other parasitic effects impressed on the photomultiplier output signal by source other than the return light must be kept to 1mv or less, a demanding requirement.

B-4. Experimental Performance Data

The magnitude of the reflectivity error, termed "walk" in the constant-fraction discriminator, is plotted in Fig. B-7 for optimum adjustment of gain and delay time of the discriminator. In Fig. B-7, Test 1 was performed with an electrical attenuator at the input to the discriminator, but tests 2 and 3 were made by ranging to a series of graduated grey-scale cards with varying reflectivity, but fixed range, 160 cm for test 2 and 307 cm for test 3.

The variation of two orders of magnitude in reflected intensity shown in Fig. B-7 is the desired amplitude range, one that might be encountered in

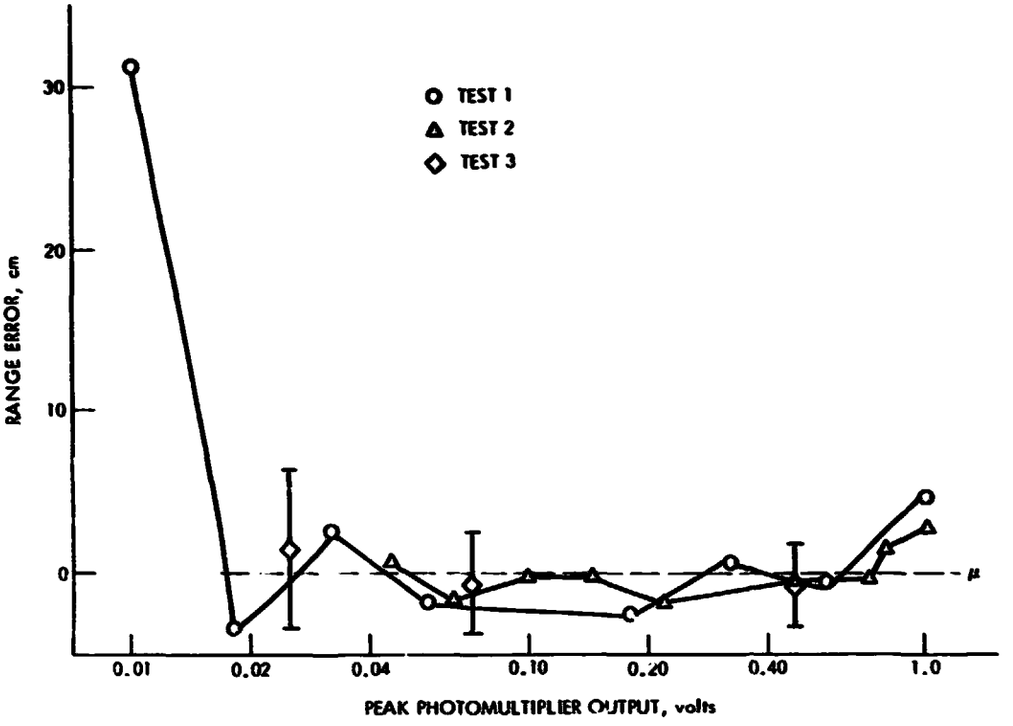

Figure B-7. Change in Measured Range as a Function of Reflected Light Intensity

practice from random objects. The black to white range for paint is somewhat less, perhaps 30 to 1, and the range of reflectivity of the most common rocks is considerably less, perhaps 5 to 1 (Ref. 33). The intensity-dependent range variation obtained from the data of Fig. B-7 is approximately 2 cm from 18 mv to 1 v, in fairly good agreement with, but larger than, the manufacturer's walk specification of 0.11 ns (1.5 cm) over an input range from 10 mv to 1 v. We were not able to extend the useful range down to 10 mv, the lower limit of constant fraction discriminator sensitivity, without an undesirably large error. The upper limit of pulse height was set by the photomultiplier, not the discriminator.

In addition to the "walk" error, a range determination is subject to uncertainty due to electronic noise. The significant noise sources are photon noise from the photodetector, a variable depending on intensity of both laser pulse and background light, and electronic noise in the critical timing

circuits. The equivalent input noise of the time to pulse height converter, as quoted by the manufacturer, is 0.15 cm (10 ps from Ref. 32). Figure B-8 shows measured equivalent range noise input of the LRF as a function of the time constant of a low-pass RC filter on the analog output signal. Figure B-9 shows a histogram for 310 raw (not averaged) range data points as read to computer memory after digitizing. The rms spread of the 310 points, collected in less than 1 sec, predicts a repeatability of their average of 0.15 cm 1σ, in reasonable agreement with figure B-8.

An important conclusion from these data is that the noise fluctuations vary, as expected, with the square root of the averaging time. With sufficient averaging time ($\gtrsim$ 0.01 sec), noise fluctuations can be made negligible compared to the reflectivity "walk" error. On the other hand, if data must be collected faster, or if one is interested in larger ranges (>3m), noise may become the significant limitation on accuracy of a single datum.

The third type of error, linearity, in principle is expected to be small because of LRF essentially measures of small difference between two large

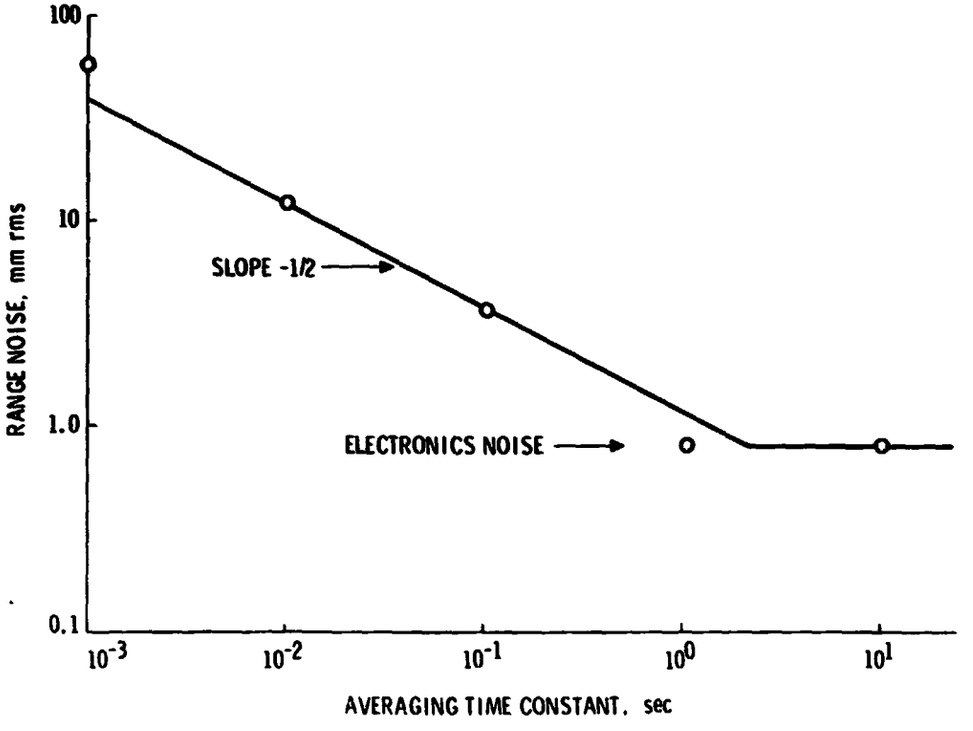

Figure B-8. Range Noise vs Averaging Time Constant

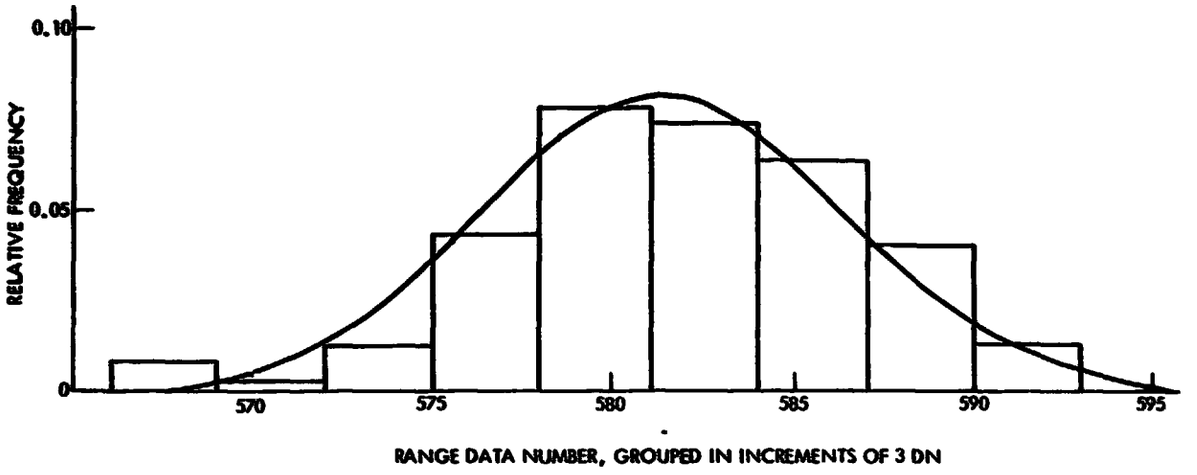

Figure B-9. Distribution of LRF Output Data Number (DN) from Fixed Target (Multipoint Averaging Removed)

delay times and the time-to pulse height converter has good linearity. However, secondary effects such as inverse square intensity variation or parasitic ringing at the constant fraction discriminator input can cause non-linearity. A measurement of overall non-linearity (Fig. B-10) indicates a linearity error of $\pm$1.5 cm over the range from 100 to 260 cm, confirming that non-linearity should not be a limiting factor.

The above tests were made inside, under normal room light conditions. Further limitation is expected from background light in direct sunlight, but fairly extensive experience with military forms of single pulse solid state laser range finding instruments has been reported. It indicates that with appropriate optical filtering, performance will not be greatly affected. (See Ref. 14). In sunlight, background light will be the limiting noise source, and no advantage from lower detector noise would be enjoyed by a photomultiplier when compared to an avalanche photodiode.

B-5. Angular Pointing Error

An experiment was performed to determine the angular pointing accuracy of the gimballed mirror and stepper motor combination. Such an error results from non-concentricity of gears and pinions, eccentricity of bearings, and frictional drag.

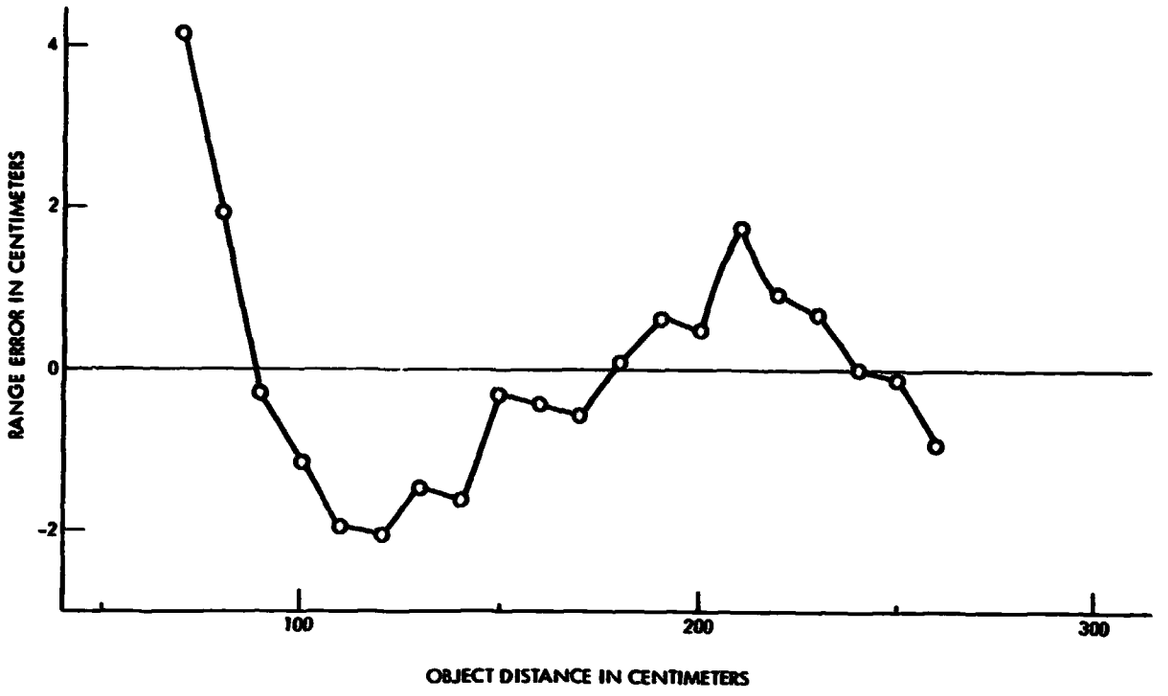

Figure B-10. Measured LRF Linearity Error

The rangefinder was mounted to an accurate dividing-head, and the gimballed mirror of the laser rangefinder was rotated through a pre-determined angle with its stepper motor. Then, using the dividing head, the rangefinder body was rotated back until the mirror was returned to its original position. This was repeated until the entire angular range had been traversed. A Wild theodolite was set up to look at its own image in the gimballed mirror, using a fine thread stretched across its objective as a target. Once set up, the theodolite was not moved until the experiment was completed.

For the azimuth test, the mirror was rotated through its total range in 19 steps of approximately 18.5° per step, going first from left to right. When the limit was reached, the same points were measured in a reverse direction. Elevation accuracy was tested in the same way by mounting the rangefinder on its side, using fifteen stepping increments of approximately 2.4° each.

Figure B-11 shows the results of the azimuth test, where mirror position θ is given by $\theta = kn +$ where k and c are constants and n is the stepper motor step number. Here $k_{measured} = 5.4011$, $k_{calculated} = 5.4024$ (from gear ratios) and a measure of hysteresis, $C_{left} - C_{right} = 0.815$ milliradians. The error $\theta_{obs} - \theta_{calc}$ has a periodic pattern that can be explained by a slightly oval shape of a sleeve bearing which was installed on the azimuth axis at the time of this test. There are two positions of the mirror, 180° apart, where the error goes through a maximum. A non-concentric gear would exhibit a period of 360°. The difference between C_{right} and C_{left} was, at first, thought to have been caused by a lack of spring tension in the anti-backlash gear, but this proved to not be the case. It, therefore, must be due to the effect of drag on the normal indexing position of the stepping motor.

Figure B-12 is a plot of elevation error. Here $k_{measured} = 2.8868$, $k_{calculated} = 2.8858$ and $\Delta C = 0.15$ milliradians. No periodic pattern traceable to a bearing defect exists here.

The azimuth data were obtained with a sleeve bearing configuration which has since been replaced by a ball bearing with much lower friction. Therefore the hysteresis observed should no longer be present. The indicated error in azimuth position is ± 0.5 mrad, and the elevation error is about 0.4 mrad, including hysteresis. Both these errors correspond to the order of 1-3 mm at the target. We can conclude that pointing errors are negligible in comparison with the range error.

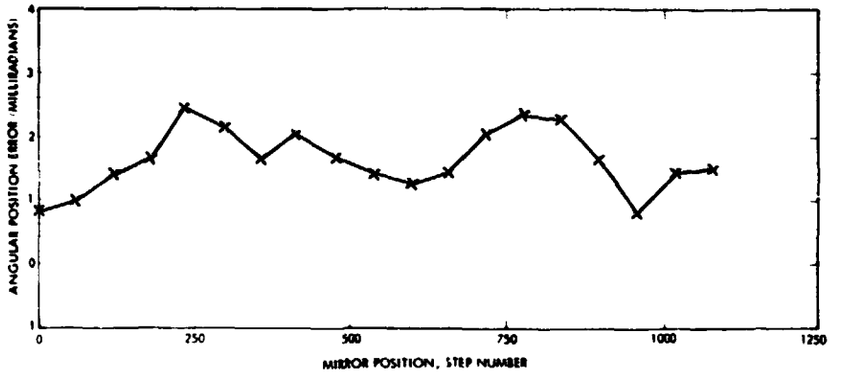

Figure B-11. Azimuth Pointing Error vs Mirror Position

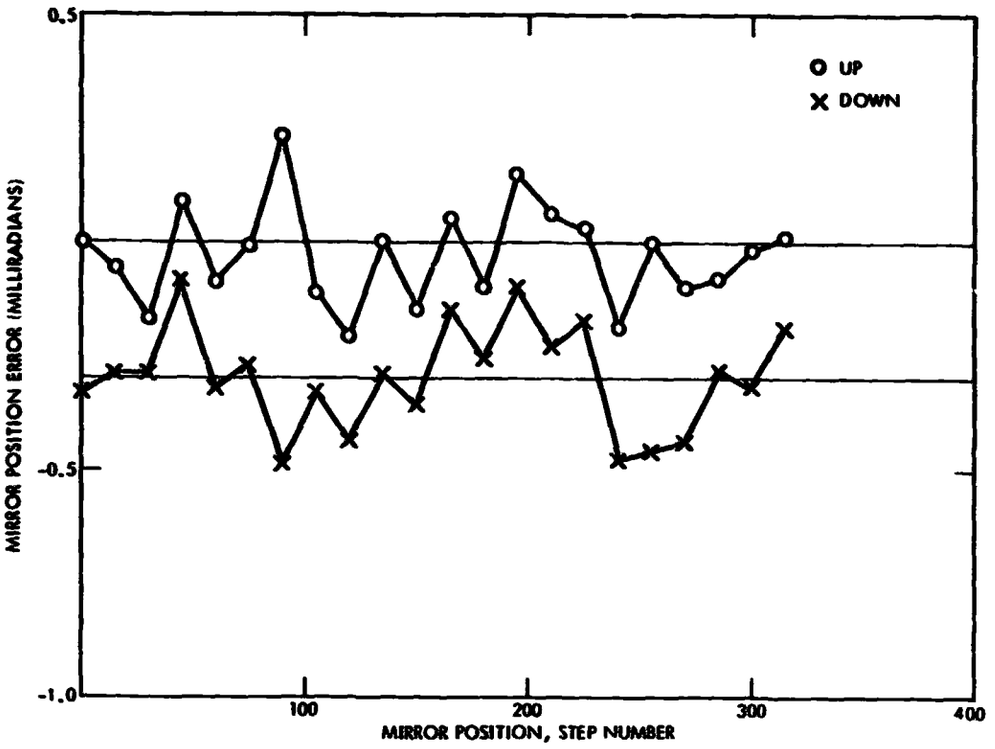

Figure B-12. Elevation Pointing Error vs Mirror Position

The laser source is imaged on the target by a lens, so the line-shaped laser spot has a finite size, 7 mm long at 2 meters. f the collimating lens is focused for a distance other than the actual target distance, the illuminated spot will appear as a larger blur circle. The lateral size of the laser spot would become a limit on the angular resolution of the LRF, though not affecting angular pointing accuracy.

In addition, a parallax effect exists because the laser and detector lens axes are not collinear. The parallax creates a predictable range dependent lateral offset of the laser image, since the beam is not emitted from the center of the gimballed mirror. Both defocusing and the lateral parallax error are of comparable magnitude, roughly 1 cm per meter displacement from a 3m focal distance.

APPENDIX C
REVISED USER'S GUIDE TO LRF SOFTWARE

LRFDOC

REVISED USER'S GUIDE TO LRF SOFTWARE. NS.LRFDOC 7/2/76

A FORTRAN AND ASSEMBLY LANGUAGE PROGRAM TO RUN THE LASER AND PAN/TILT HEAD THAT IS TOTALLY CONTAINED IN THE SPC-16 HAS BEEN DEVELOPED AND TESTED. THE PROGRAM CONSISTS OF THE 10 SUBROUTINES LRF, LRFD, LRESET, RND, SLPNT, POINT, LCAL, CONVRT, SCANL, AND UNPNT (ON LB & DSKA:UL) STORED IN SOURCE CODE ON DSKA:NS FILES RLAS00,...,RLAS08 AND RLAS11, RESPECTIVELY. THE SUBROUTINES ARE CONSIDERED AS A TOTAL UNIT TOGETGER WITH A TELETYPE-ORIENTED DRIVER NS.RLASER AND TWO ADITIONAL SUBROUTINES (SCNREC AND SCANV, ON NS.RLAS09-10). THE SUBROUTINES LOAD IN 2811 ON DC.RLASER. WITHOUT THE TELETYPE DRIVER AND THE TWO EXTRA SUBROUTINES, THE LASER PROGRAMS LOAD IN 158E. A SCANNER FOR THE IN-MOTION VEHICLE (SCANV, ON NS.RLAS10) CAN BE USED SEPARATELY AND REQUIRES 0806 (=2822) WORDS. A PDP-10 DRIVER COULD BE DEVELOPED SHOULD THE NEED ARISE. THE SUBROUTINES CAN, OF COURSE, BE LOADED WITH ANY OTHER MAIN PROGRAM, THEREBY PUTING THE LASER AT THE SERVICE OF THE CALLING SYSTEM.

THE SOFTWARE ACCEPTS 10 MAIN COMMANDS, GIVEN AS THE INTEGERS 0 TO 9 AND SUMMARIZED IN TABLE 1. I/PUT AND OUTPUT (ARGUMENTS AND DATA) ARE DONE VIA A 16-WORD REAL ARRAY (BUF). THE PROGRAM IS CALLED BY REPEATED EXECUTION OF THE STATEMENT

CALL LRF(INTEGER COMMAND, 16-WORD REAL ARRAY)

THE CONTENTS OF THE ARRAY ARE SPECIFIED BELOW. NO INITIALIZING COMMANDS AT THE MONITOR LEVEL ARE REQUIRED (THOUGH IF RUNNING FROM TELETYPE, YOU MAY WANT TO ASSIGN 5=LP FOR SCANLINE OUTPUT). THE NAMED COMMON BLOCK LRFDTA, WITH 2 REALS AND 1000 INTEGERS (THE 200 X 5 INTEGER ARRAY IRANGE) MUST BE DECLARED IN THE MAIN OR CALLING PROGRAM. LRF MUST BE CALLED THE FIRST TIME WITH A NEGATIVE COMMAND; A GOOD DEFAULT VALUE, THE ONE USED BY THE TELETYPE DRIVER, IS -1. (SEE TABLE 1 FOR MORE DETAIL)

ALL I/O IS IN INCHES OR INTEGER STEPS (SEE BELOW). ERROR FLAGS, DESCRIBED IN TABLE 2, APPEAR IN BUF(16). ON ERRORS 1,2,3,5,6,&7, A RESET (COMMAND 1) SHOULD BE DONE.

* * * * * * * * *

COORDINATE SYSTEMS

LASER STEP (LST): (AZ,EL,RDN). 31 .LE. AZ .LE. 1023 730=AZ RESET
INCREASING AZ MOVES LRF TO LEFT.
100 .LE. EL .LE. 857 738=EL RESET
INCREASING EL MOVES BEAM (MIRROR) DOWN
0 .LE. RDN .LE. 1023. RDN LINEARLY PROPORTIONAL TO RANGE.

ROTATED PAN/TILT (RPT). (X,Y,Z) IN INCHES, CENTERED AT LRF AND IN FRAME ALIGNED WITH CURRENT PAN/TILT POSITION X=LINE OF SIGHT OF P/T, Y ALONG TILT AXIS, Z ALONG PAN AXIS.

ARM : STANDARD (X,Y,Z) MANIPULATOR BASE FRAME, IN INCHES

* * * * * * * * * *

TABLE 1. COMMANDS
(ALL ERROR FLAGS IN BUF(16), SEE TABLE 2)

LESS THAN ZERO. THE LRF REQUIRES CALIBRATION EVERY SO OFTEN. THE SCALE FACTOR (CONVERTING VOLTAGE TO RANGE) REMAINS FAIRLY CONSTANT, BUT THE OFFSET DRIFTS AS THE INSTRUMENT WARMS UP. THUS THE SOFTWARE IS EQUIPPED TO AUTOMATICALLY RECALIBRATE EVERY 300 SECONDS. WITH AN INITIAL COMMAND OF N=-300 OR LESS, THE INSTRUMENT WILL RECALIBRATE NOW AND THEN EVERY N SECONDS. WITH AN INITIAL COMMAND OF -1, THE INSTRUMENT WILL ONLY BE CALIBRATED INITIALLY; AUTOMATIC RECALIBRATION WILL NOT OCCUR ANY OTHER NEGATIVE COMMAND WILL LEAVE THE LRF RECALIBRATING AT ITS DEFAULT INTERVAL (300 SECONDS). (RECALIBRATION CAN BE SPECIFICALLY ORDERED WHEN DESIRED VIA COMMAND 4)

```
0     THIS COMMAND IS REALLY A SERIES OF VERY SPECIFIC SUBCOMMANDS
      THAT WILL SELDOM, IF EVER, BE USED.  THEY ARE OFFERED FOR
      COMPLETENESS.  THE SUBCOMMAND IS READ FROM BUF(13); WITH
      THE TELETYPE DRIVER, INPUT THE SUBCOMMAND AS A SEPARATE LINE.

      SUBCOMMAND
      0     RESETS ELECTRONICS
      1     TEST IF SCAN BUSY; TRUE(=1) OR FALSE(=0) RETURNED IN BUF(13)
      2     TEST IF POWER ON;                                          .
      3     TEST IF DATA READY;                                        .
      4     RESET ELEVATION (TO 738)
      5     RESET AZIMUTH (TO 730)
      6     EL SCAN TO ARG INPUT ON SEPARATE LINE (TELETYPE DRIVER) OR
            FROM BUF(5).  ARGS IN LST COORDS.  OUTPUT RDN IN IRANGE.
      7     AZ SCAN TO ARG INPUT ON SEPARATE LINE (TELETYPE DRIVER) OR
            FROM BUF(4).  ARGS IN LST COORDS.  OUTPUT RDN IN IRANGE.
      8     EL SLEW TO ARG INPUT FROM SEPARATE LINE OR BUF(5) IN LST,
            OUTPUT RDN IN BUF(6).
      9     AZ SLEW TO ARG INPUT FROM SEPARATE LINE OR BUF(4) IN LST,
            OUTPUT RDN IN BUF(6).

1     LASER RESET.  NO ARGUMENTS.

2     SLEW TO AZ,EL,N.  INPUT ON SEPARATE LINE (TTY) OR FROM BUF(4),
      BUF(5), BUF(13), WHERE N=NUMBER OF READINGS TO BE TAKEN.  AVERAGE
      RANGE READING ENTERED IN BUF(6).  IF N>1, SIGMA**2 ENTERED INTO
      BUF(13).

3     OPERATES PAN/TILT.  A SUBCOMMAND IS ENTERED ON A SEPARATE LINE(TTY)
      OR IN BUF(13).  IF =3, CURRENT P/T STEPS READ INTO BUF(14) (TILT)
      AND BUF(15) (PAN); IF =7, MOVES TO P/T STEPS INPUT ON SEPARATE
      LINE TTY) OR IN BUF(14),BUF(15).  IN EITHER CASE, LINE OF SIGHT
      OF P/T HEAD READ INTO BUF(10)-BUF(12).

4     RECALIBRATES LRF.

5     CONVERTS FROM ONE COORDINATE SYSTEM TO ANOTHER.  SUBCOMMAND
      ENTERED ON SEPARATE LINE (TTY) OR FROM BUF(13).  INPUT IS
      ENTERED ON SEPARATE LINE OR FROM BUF LOCATIONS GIVEN BELOW.

      SUBCOMMAND  FUNCTION      INPUT              OUTPUT
      1           LST TO ARM    BUF(1)-BUF(3)      BUF(7)-BUF(9)
      2           ARM TO LST    BUF(7)-BUF(9)      BUF(1)-BUF(3)
      3           LST TO RPT    BUF(1)-BUF(3)      BUF(7)-BUF(9)
      4           RPT TO LST    BUF(7)-BUF(9)      BUF(1)-BUF(3)
      5           RPT TO ARM    BUF(7)-BUF(9)      BUF(7)-BUF(9)
      6           ARM TO RPT    BUF(7)-BUF(9)      BUF(7)-BUF(9)

6     SCANS LINE, UP TO 200 POINTS, PUTTING RESULTS INTO IRANGE(IN
      NAMED COMMON BLOCK LRFDTA).  A SUBCOMMAND IS ENTERED IN BUF(13)
      OR ON A SEPARATE LINE (TTY); IF =1, INPUTS ARE IN LST; IF =2 OR 4,
      INPUTS ARE IN ARM; IF =3, INPUTS ARE IN RPT COORDINATES.
      (IF = 4, MOVES PAN/TILT TO MIDPOINT OF LINE BEFORE STARING SCAN.)
      THEN, ON ANOTHER LINE (TTY), OR IN BUF(1)-BUF(6) (IF LST),
      OR IN BUF(7)-BUF(12) (IF ARM OR RPT), THE SCAN BOUNDARIES ARE
      ENTERED.  THE FIRST THREE NUMBERS GIVE THE COORDINATES OF THE
      FIRST ENDPOINT, THE SECOND THREE THOSE OF THE OTHER ENDPOINT.
      UP TO THE FIRST 200 POINTS OF THE LINE WILL BE SCANNED.  THE
      NUMBER OF POINTS SCANNED IS RETURNED IN BUF(14).  IF 200 POINTS
      ARE SCANNED, THEN THE BEGINNING AND END OF THE REST OF THE LINE
      ARE RETURNED IN BUF(1)-BUF(6); REPEATING THIS COMMAND WITH
      SUBCOMMAND (BUF(13)) = 1 WILL FINISH THE SCAN.  THE 200 X 5
      ARRAY IRANGE (IN THE NAMED COMMON BLOCK LRFDTA) CONTAINS ON
      RETURN, IN EACH ROW, THE LASER STEPS (AZ,EL) AND THE SCANNED
      (X,Y,Z) POSITION IN ARM COORDINATES.  WITH THE TTY DRIVER,
      IRANGE IS OUTPUT ON LU5.  A ONE-POINT LINE WILL BE SCANNED.

7     TELETYPE DRIVER ONLY.  RAMTEK MUST BE ON; INTENSITY=ELEVATION.

      SCANS A RECTANGULAR REGION, LOOKING FOR THE TALLEST OBJECT IT CAN
      FIND.  THE SUBCOMMAND, ENTERED ON A SEPARATE LINE OR IN BUF(13),
      SPECIFIES INPUT COORDINATES:  1=LST, 2=ARM, 3=RPT.  THEN, IN
      BUF(1)-BUF(12) OR ON THE NEXT LINE, THE FOUR CORNERS ARE INPUT.
      THE LAST SIX INPUTS SPECIFY THE FIRST LINE SCANNED, THE SECOND
      SIX THE FIRST LINE SCANNED.  INTERMEDIATE LINES PARALLEL TO THESE
      ARE ALSO SCANNED.  ON RETURN, IF NO OBJECT IS FOUND, BUF(15)=0.
      OTHERWISE, BUF(15)=1 AND BUF(4)-BUF(6) CONTAIN THE ARM (X,Y,Z)
      OF THE OBJECT'S CENTER AND BUF(10) ITS ORIENTATION.  FURTHERMORE,
      WITH THE TTY DRIVER, THESE FOUR NUMBERS ARE WRITTEN ON LU14.
```

0 TELETYPE DRIVER ONLY. CAN ALSO BE CALLED SEPARATELY AS SCANV; ONLY SCANV, RPOINT, LRESET, AND LRFD NEEDED.

VEHICLE MOTION SCAN. SETS UP LASER SCAN OF AREA 10 FEET IN FRONT OF VEHICLE (10 FEET FROM LRF), FROM X=-50 TO X=20 AND BACK, LOOKING FOR VEHICLE OBSTACLES. THE FIRST INPUT, ON A SEPARATE LINE OR IN BUF(13), IS A SUBCOMMAND SPECIFYING WHAT IS TO BE DONE: -10 PREPARES FOR SCAN BY MOVING THE LASER AND PAN/TILT TO APPROPRIATE START POSITIONS; 0 STARTS THE SCAN AND RETURNS TO THE CALLING PROGRAM; +10 PROCESSES THE SCAN DATA. ON OUTPUT, BUF(14) PROVIDES STATUS (10=STILL SCANNING, 9=PROCESSING FINISHED). BUF(16) CONTAINS THE USUAL ERROR MESSAGES, BUT BUF(15) CONTAINS THE WORD NUMBER OF IRANGE WHERE THE ERROR OCCURED. IRANGE CONTAINS THE RANGE DATA. IF THE PROCESSING FINISHES WITHOUT ERROR, BUF(15) INDICATES THE PRESENCE(1) OR ABSENCE(0) OF AN OBJECT. IF AN OBJECT IS FOUND, ITS LST COORDINATES ARE GIVEN IN BUF(1)-BUF(3).

9 STOPS PROGRAM AFTER CLOSING LRF MIRROR.

* * * * * * * * * *

TABLE 2: ERROR CODE
(IN BUF(16))

0 OK
1 AZ LOWER LIMIT VIOLATED
2 AZ UPPER LIMIT VIOLATED
3 AZ SKIP STEP
4 RDN<0 (POWER SUPPLY OFF, MEANINGLESS RANGE READING)
5 EL LOWER LIMIT VIOLATED
6 EL UPPER LIMIT VIOLATED
7 EL SKIP STEP
8 POINT SUBROUTINE ERROR (PAN/TILT)
9 LRF MAY NOT BE "WARM" YET, SIGMA(*2)1
10 UNSPECIFIED PROBLEM IN LRF--NOT GETTING AS MANY READINGS AS COMMANDED ON SLEW
11 CLOCK OFF
12 TOO FAR FOR GOOD DATA
15 COMMAND ERROR
16 SCAN INPUT ERROR
22 IN CONVERSION, RESULTING AZ STEP WOULD VIOLATE LIMIT
23 IN CONVERSION, RESULTING EL STEP WOULD VIOLATE LIMIT
24 IN CONVERSOON, RESULTING RANGE NUMBER WOULD VIOLATE LIMIT

* * *

DEMO

SPC-16 ONLY
FINDS ROCK, STICKS INTO NEST ON LASER DISK

CC=NS.LRF2

* * * *

HARDWARE/ELECTRONICS SETTINGS

"GAIN"--SET TO 3
"RT REJECT"--SET TO 1
"RANGE"--SET TO 50 (IF DISTANCES OVER 20 FEET ARE TO BE MEASURED AND NEAR OBJECTS ARE NOT OF INTEREST, CAN SET TO 250 IF RECALIBRATE.

* * * * *

END

APPENDIX D
LRF SOFTWARE FLOWCHARTS

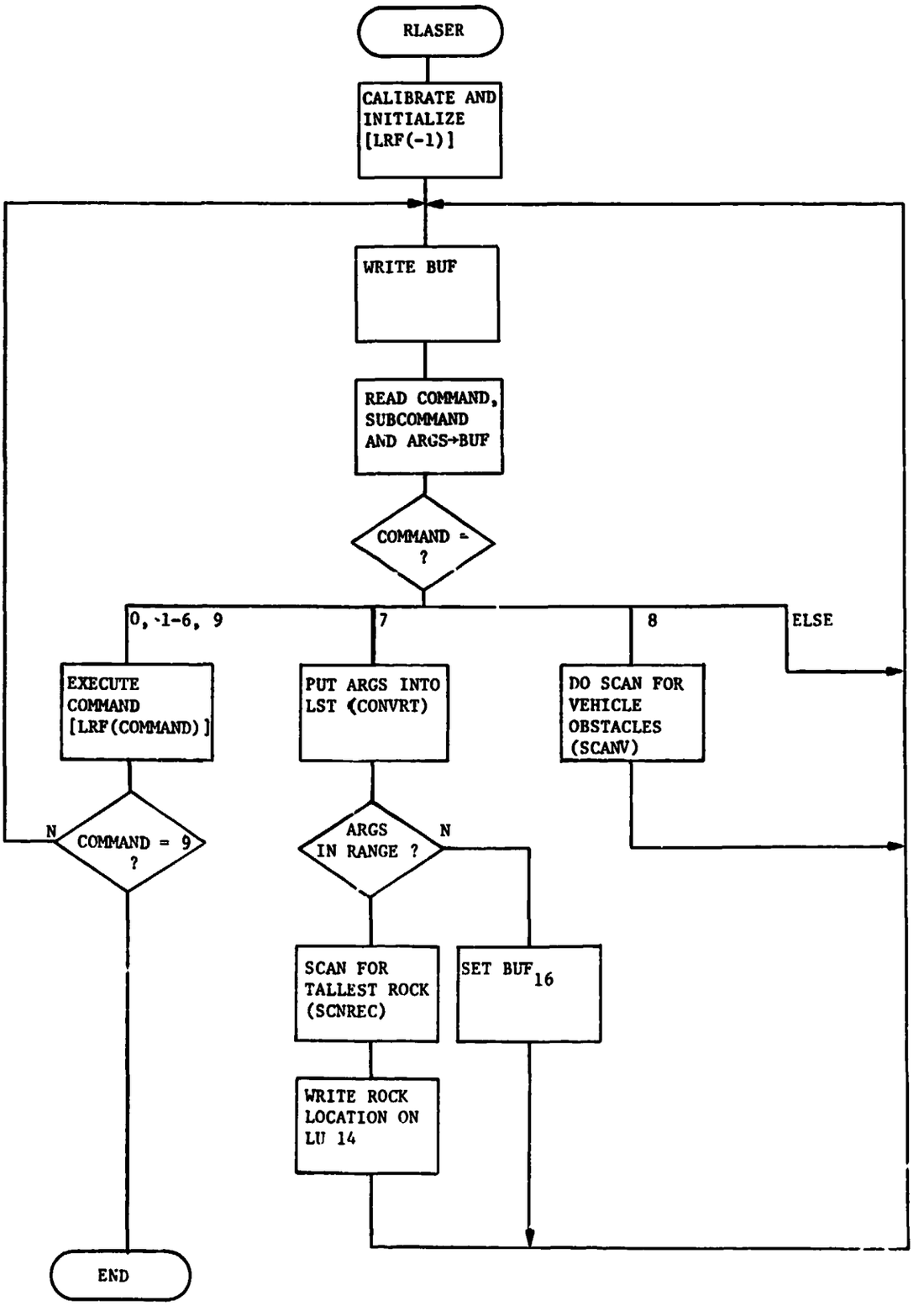
RLASER
CALIBRATE AND INITIALIZE [LRF(-1)]
WRITE BUF
READ COMMAND, SUBCOMMAND AND ARGS→BUF
COMMAND = ?
0, -1-6, 9
7
8
ELSE
EXECUTE COMMAND [LRF(COMMAND)]
PUT ARGS INTO LST (CONVRT)
DO SCAN FOR VEHICLE OBSTACLES (SCANV)
N
COMMAND = 9 ?
ARGS IN RANGE ?
N
SCAN FOR TALLEST ROCK (SCNREC)
SET BUF 16
WRITE ROCK LOCATION ON LU 14
END

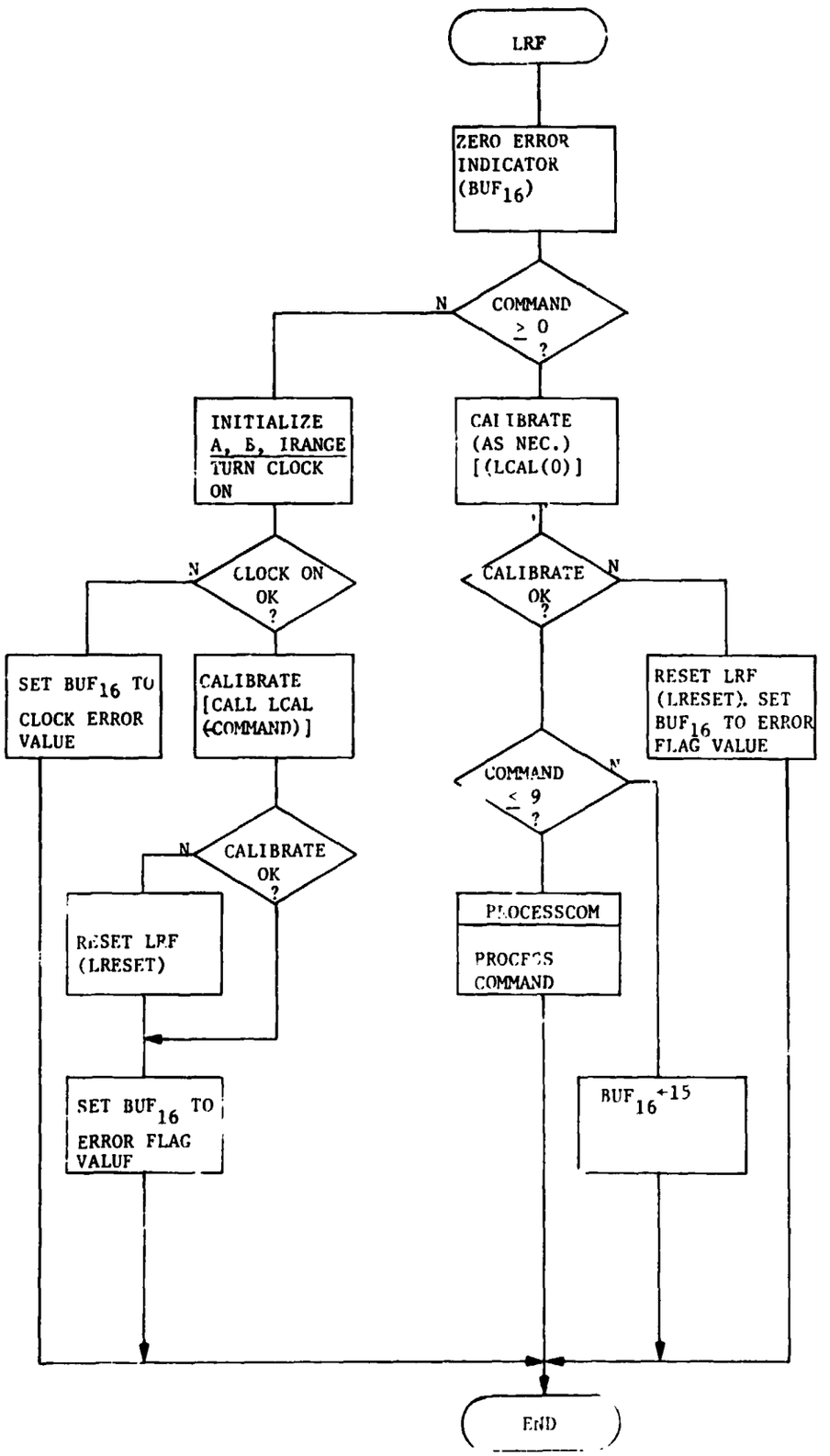
LRF
ZERO ERROR INDICATOR (BUF_{16})
COMMAND ≥ 0 ?
N
INITIALIZE A, B, IRANGE TURN CLOCK ON
CALIBRATE (AS NEC.) [(LCAL(0)]
CLOCK ON OK ?
N
CALIBRATE OK ?
N
SET BUF_{16} TO CLOCK ERROR VALUE
CALIBRATE [CALL LCAL (COMMAND)]
RESET LRF (LRESET). SET BUF_{16} TO ERROR FLAG VALUE
COMMAND ≤ 9 ?
N
CALIBRATE OK ?
N
RESET LRF (LRESET)
PROCESSCOM
PROCESS COMMAND
SET BUF_{16} TO ERROR FLAG VALUE
BUF_{16} ← 15
END

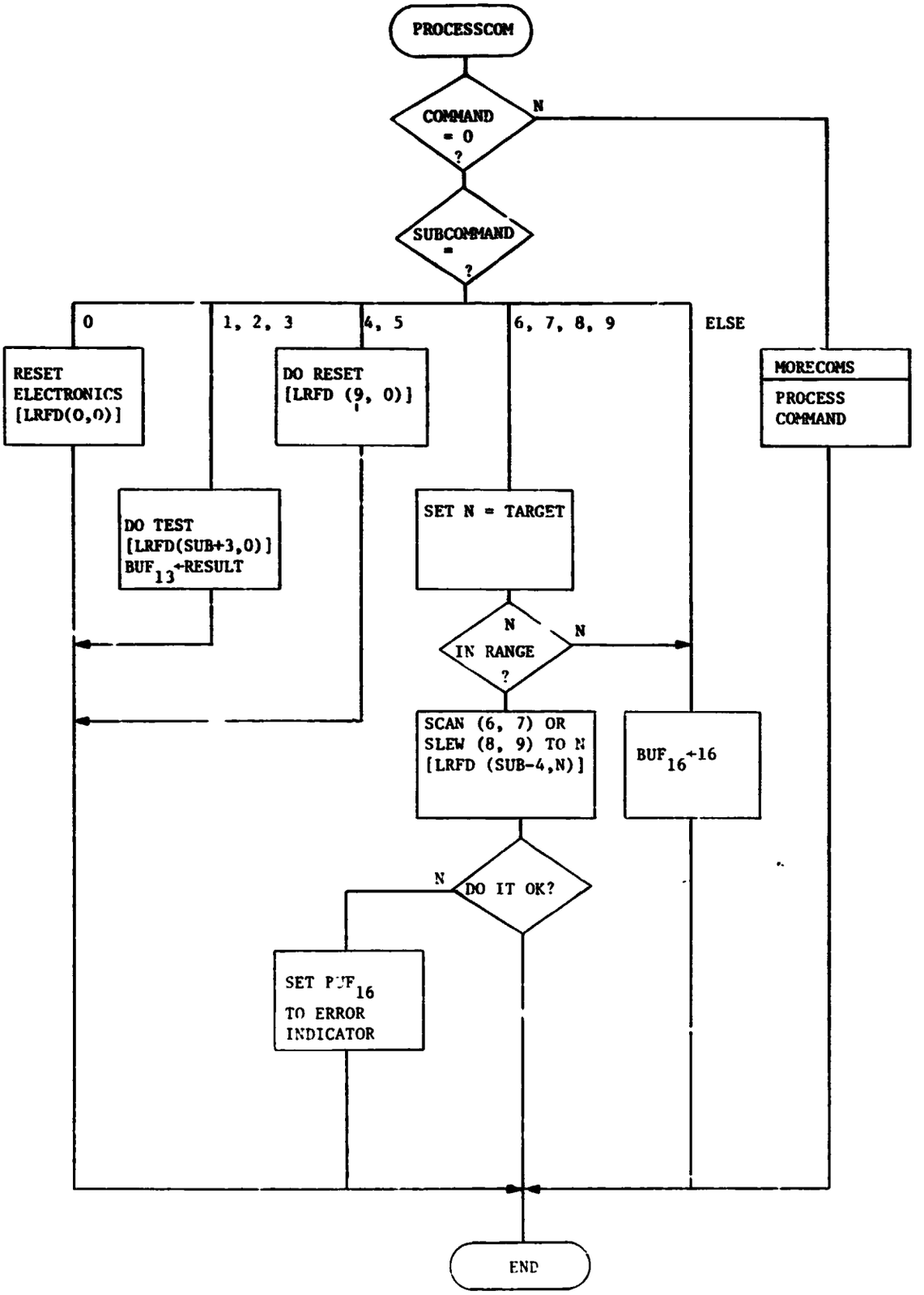
PROCESSCOM
COMMAND = 0 ?
N
SUBCOMMAND = ?
0
1, 2, 3
4, 5
6, 7, 8, 9
ELSE
RESET ELECTRONICS [LRFD(0,0)]
DO RESET [LRFD (9, 0)]
MORECOMS
PROCESS COMMAND
DO TEST [LRFD(SUB+3,0)] BUF13←RESULT
SET N = TARGET
N
IN RANGE ?
N
SCAN (6, 7) OR SLEW (8, 9) TO N [LRFD (SUB-4,N)]
BUF16←16
N
DO IT OK?
SET BUF16 TO ERROR INDICATOR
END

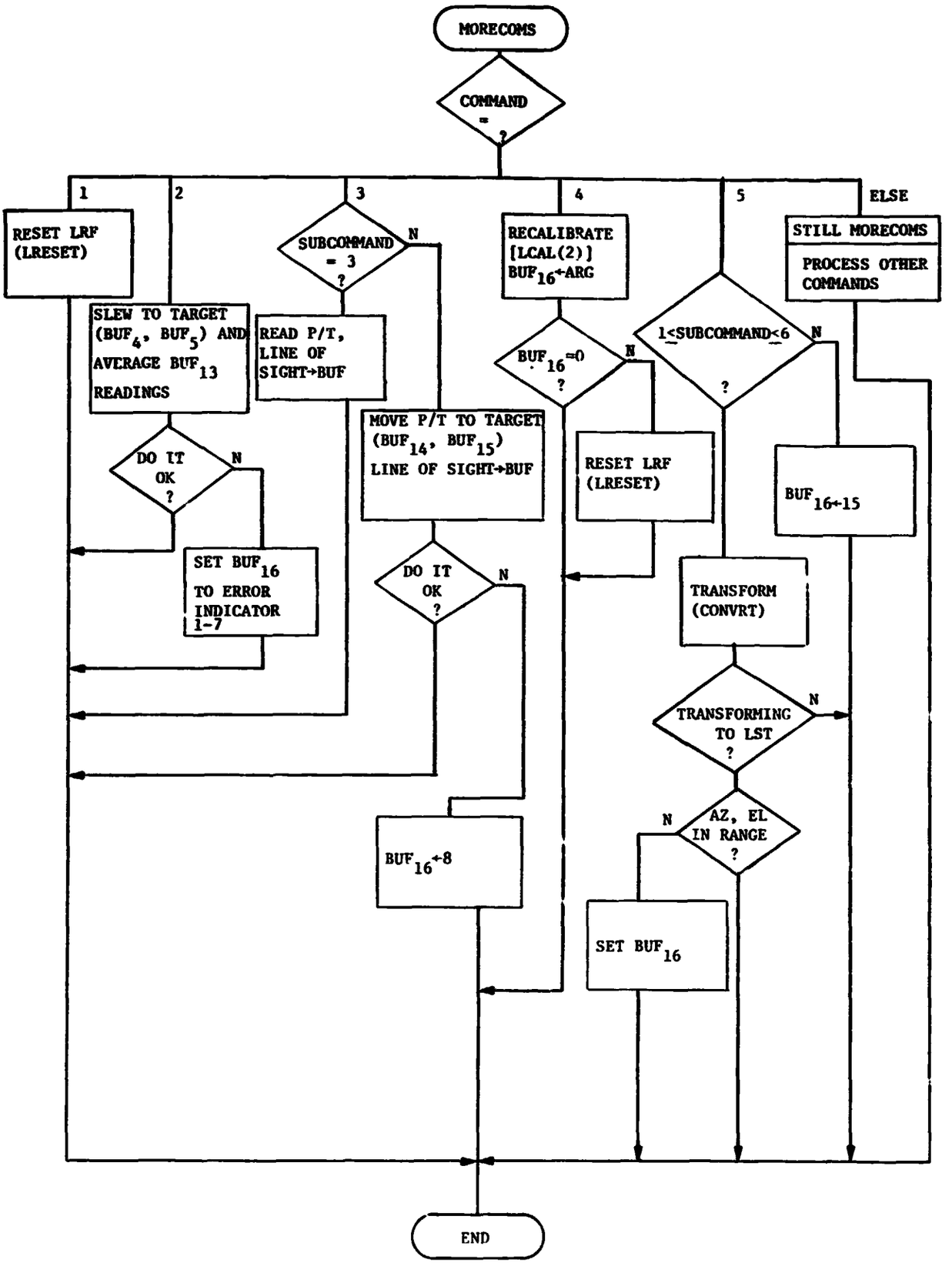
MORECOMS
COMMAND = ?
1
2
3
4
5
ELSE
RESET LRF (LRESET)
SLEW TO TARGET (BUF4, BUF5) AND AVERAGE BUF13 READINGS
SUBCOMMAND = 3 ?
N
READ P/T, LINE OF SIGHT→BUF
RECALIBRATE [LCAL(2)] BUF16←ARG
1≤SUBCOMMAND≤6 ?
N
STILL MORECOMS
PROCESS OTHER COMMANDS
DO IT OK ?
N
SET BUF16 TO ERROR INDICATOR 1-7
MOVE P/T TO TARGET (BUF14, BUF15) LINE OF SIGHT→BUF
BUF16=0 ?
N
RESET LRF (LRESET)
BUF16←15
DO IT OK ?
N
TRANSFORM (CONVRT)
TRANSFORMING TO LST ?
N
AZ, EL IN RANGE ?
N
BUF16←8
SET BUF16
END

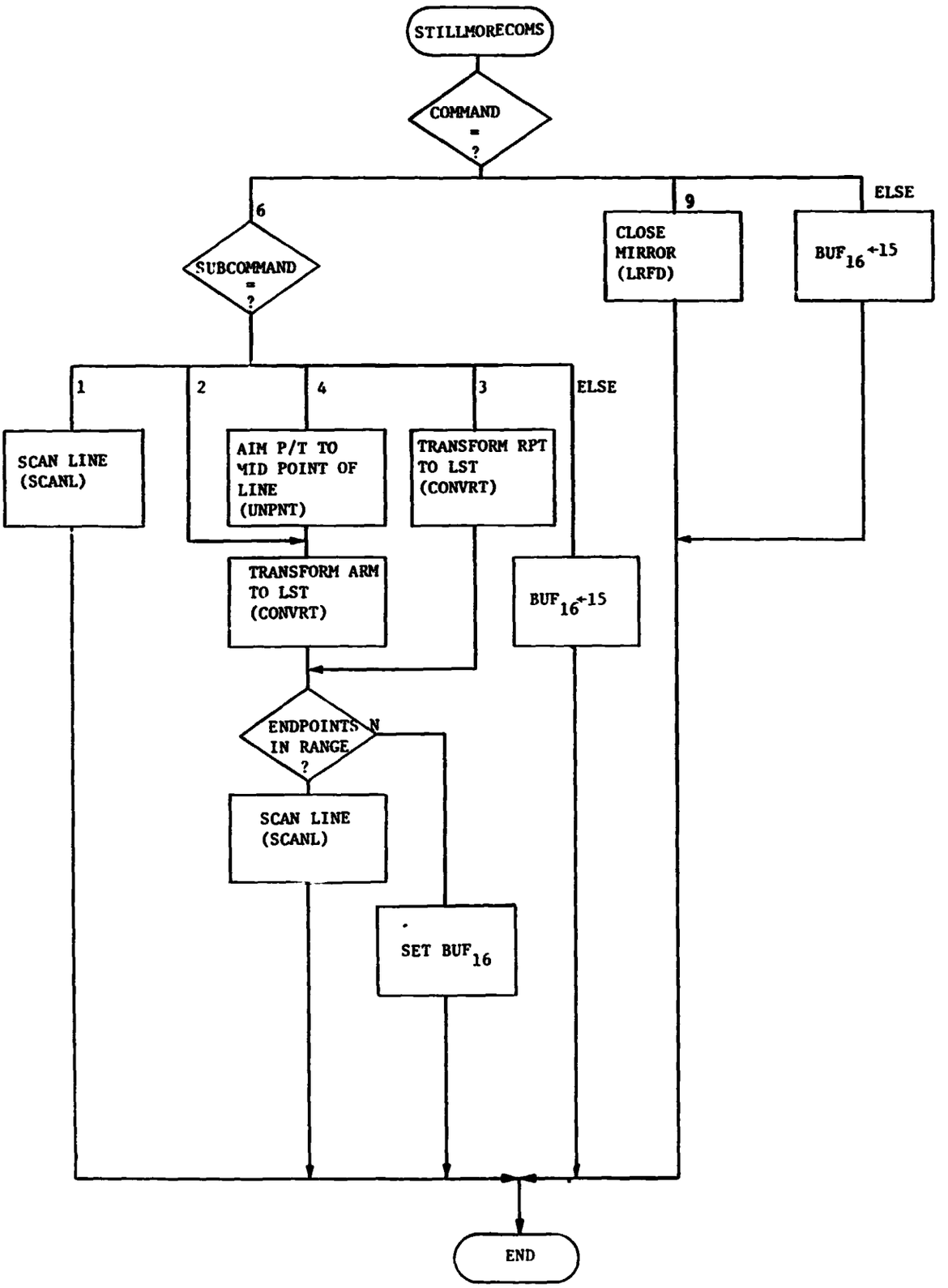
STILLMORECOMS
COMMAND = ?
6
9
ELSE
SUBCOMMAND = ?
CLOSE MIRROR (LRFD)
BUF16←15
1
2
4
3
ELSE
SCAN LINE (SCANL)
AIM P/T TO MID POINT OF LINE (UNPNT)
TRANSFORM RPT TO LST (CONVRT)
TRANSFORM ARM TO LST (CONVRT)
BUF16←15
ENDPOINTS IN RANGE ?
N
SCAN LINE (SCANL)
SET BUF16
END

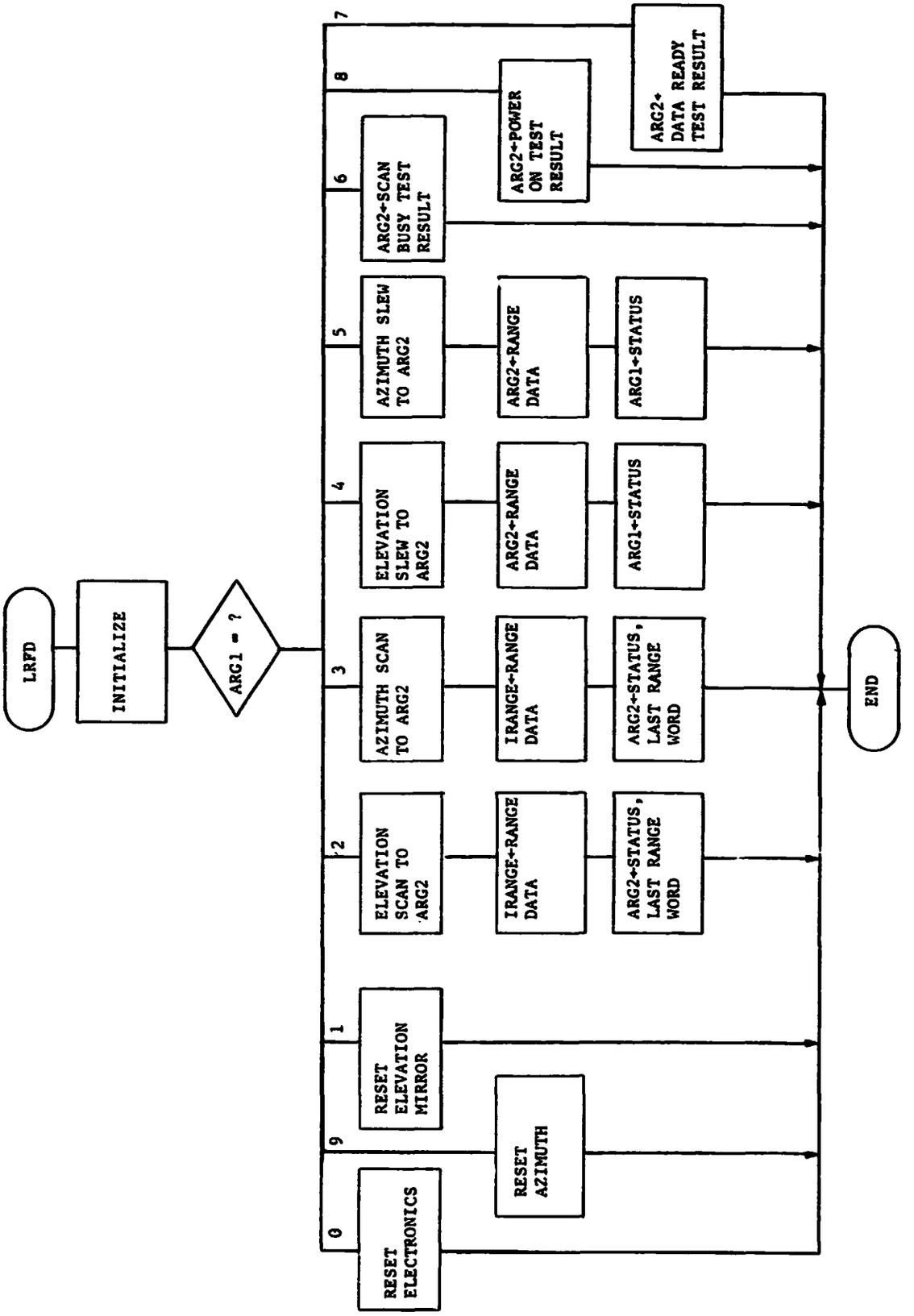
LRFD
INITIALIZE
ARG1 = ?
0
RESET ELECTRONICS
1
RESET ELEVATION MIRROR
2
ELEVATION SCAN TO ARG2
IRANGE→RANGE DATA
ARG2→STATUS, LAST RANGE WORD
3
AZIMUTH SCAN TO ARG2
IRANGE→RANGE DATA
ARG2→STATUS, LAST RANGE WORD
4
ELEVATION SLEW TO ARG2
ARG2→RANGE DATA
ARG1→STATUS
5
AZIMUTH SLEW TO ARG2
ARG2→RANGE DATA
ARG1→STATUS
6
ARG2→SCAN BUSY TEST RESULT
7
ARG2→ DATA READY TEST RESULT
8
ARG2→POWER ON TEST RESULT
9
RESET AZIMUTH
END

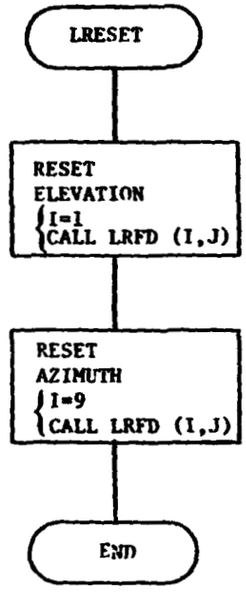
LRESET
RESET
ELEVATION
I=1
CALL LRFD (I,J)
RESET
AZIMUTH
I=9
CALL LRFD (I,J)
END

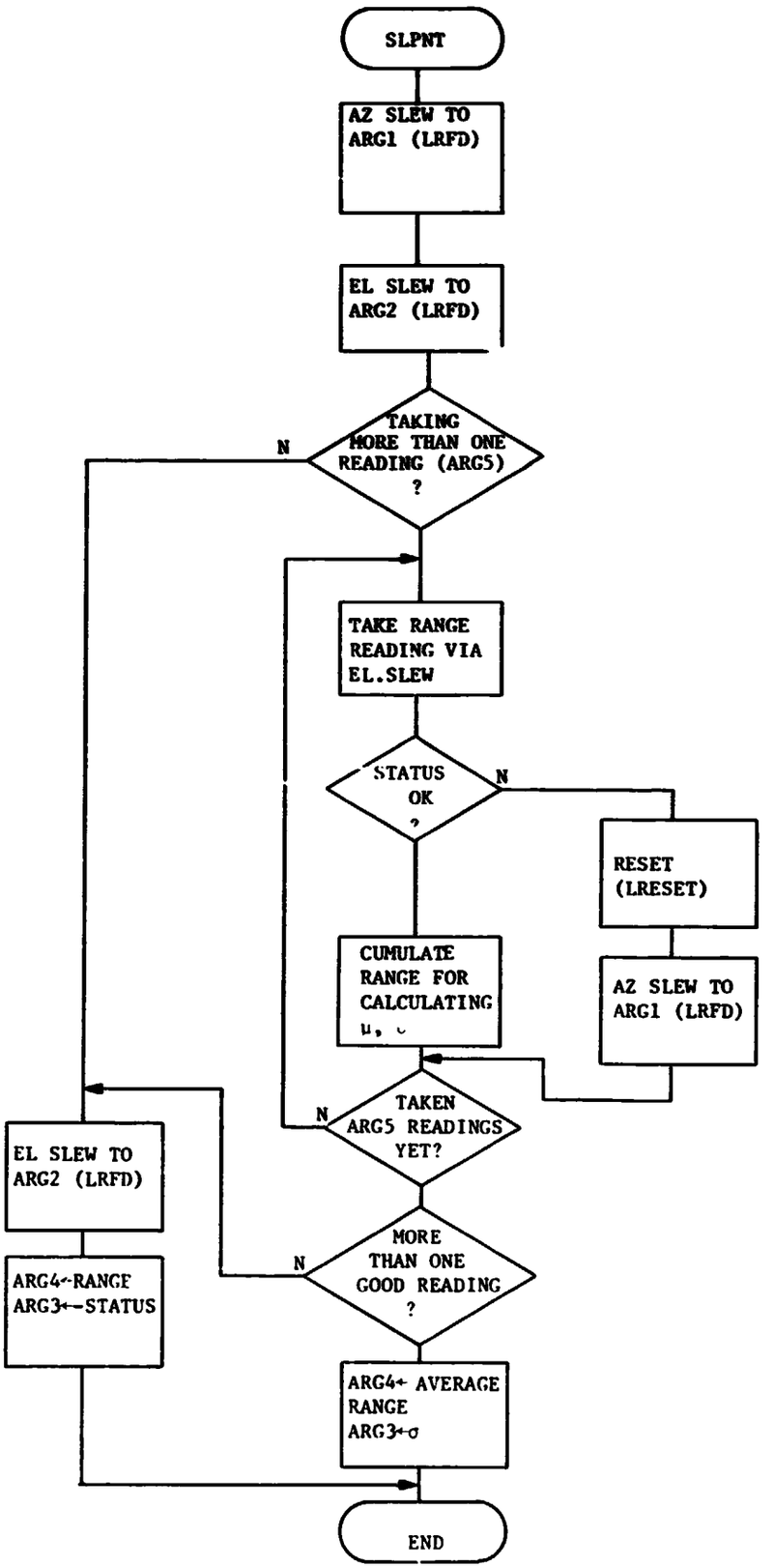
SLPNT
AZ SLEW TO ARG1 (LRFD)
EL SLEW TO ARG2 (LRFD)
TAKING MORE THAN ONE READING (ARG5) ?
N
TAKE RANGE READING VIA EL.SLEW
STATUS OK ?
N
RESET (LRESET)
AZ SLEW TO ARG1 (LRFD)
CUMULATE RANGE FOR CALCULATING μ, σ
TAKEN ARG5 READINGS YET?
N
MORE THAN ONE GOOD READING ?
N
EL SLEW TO ARG2 (LRFD)
ARG4←RANGE
ARG3←STATUS
ARG4← AVERAGE RANGE
ARG3←σ
END

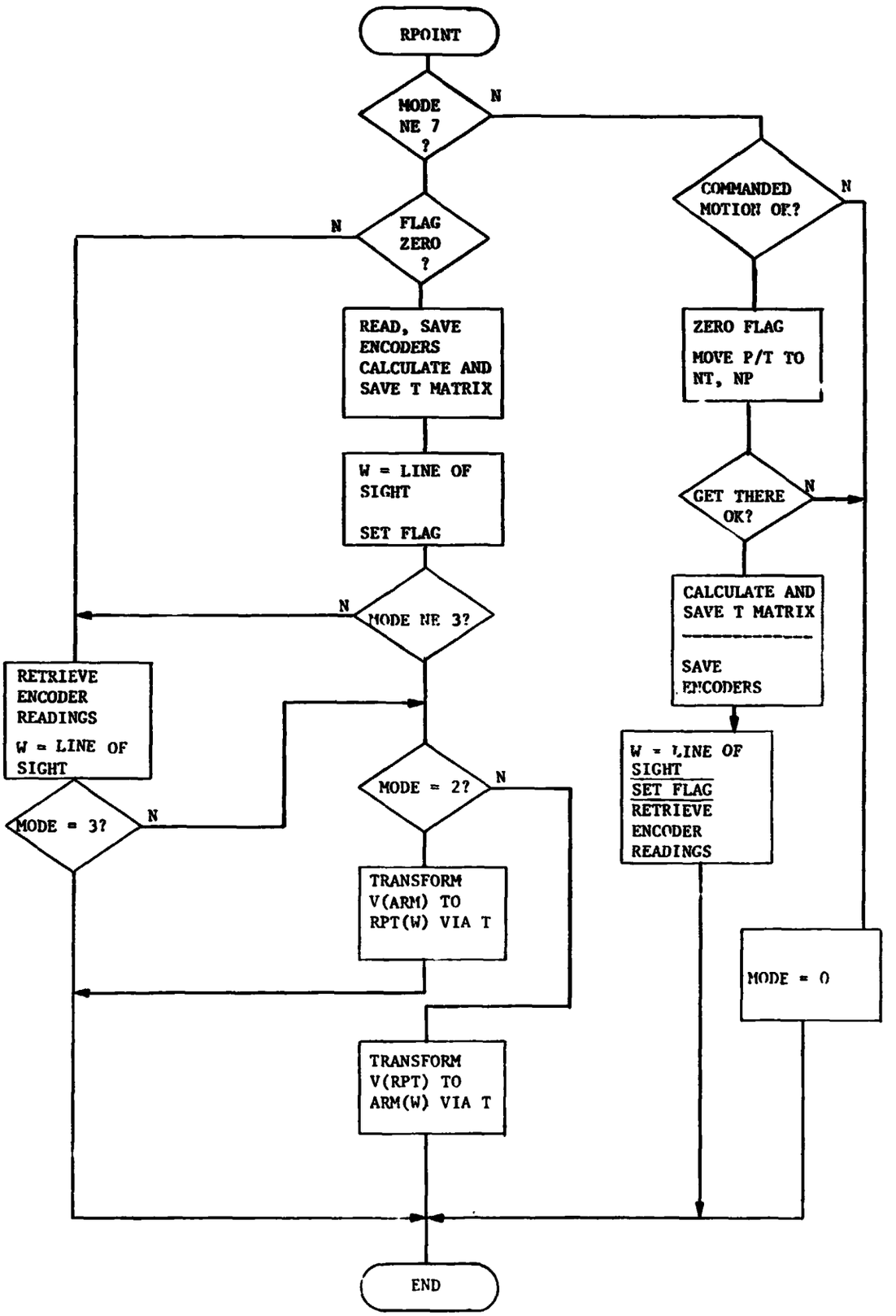
RPOINT
MODE NE 7 ?
N
FLAG ZERO ?
N
READ, SAVE ENCODERS CALCULATE AND SAVE T MATRIX
W = LINE OF SIGHT
SET FLAG
MODE NE 3?
N
RETRIEVE ENCODER READINGS
W = LINE OF SIGHT
MODE = 3?
N
MODE = 2?
N
TRANSFORM V(ARM) TO RPT(W) VIA T
TRANSFORM V(RPT) TO ARM(W) VIA T
COMMANDED MOTION OK?
N
ZERO FLAG
MOVE P/T TO NT, NP
GET THERE OK?
N
CALCULATE AND SAVE T MATRIX
SAVE ENCODERS
W = LINE OF SIGHT
SET FLAG
RETRIEVE ENCODER READINGS
MODE = 0
END

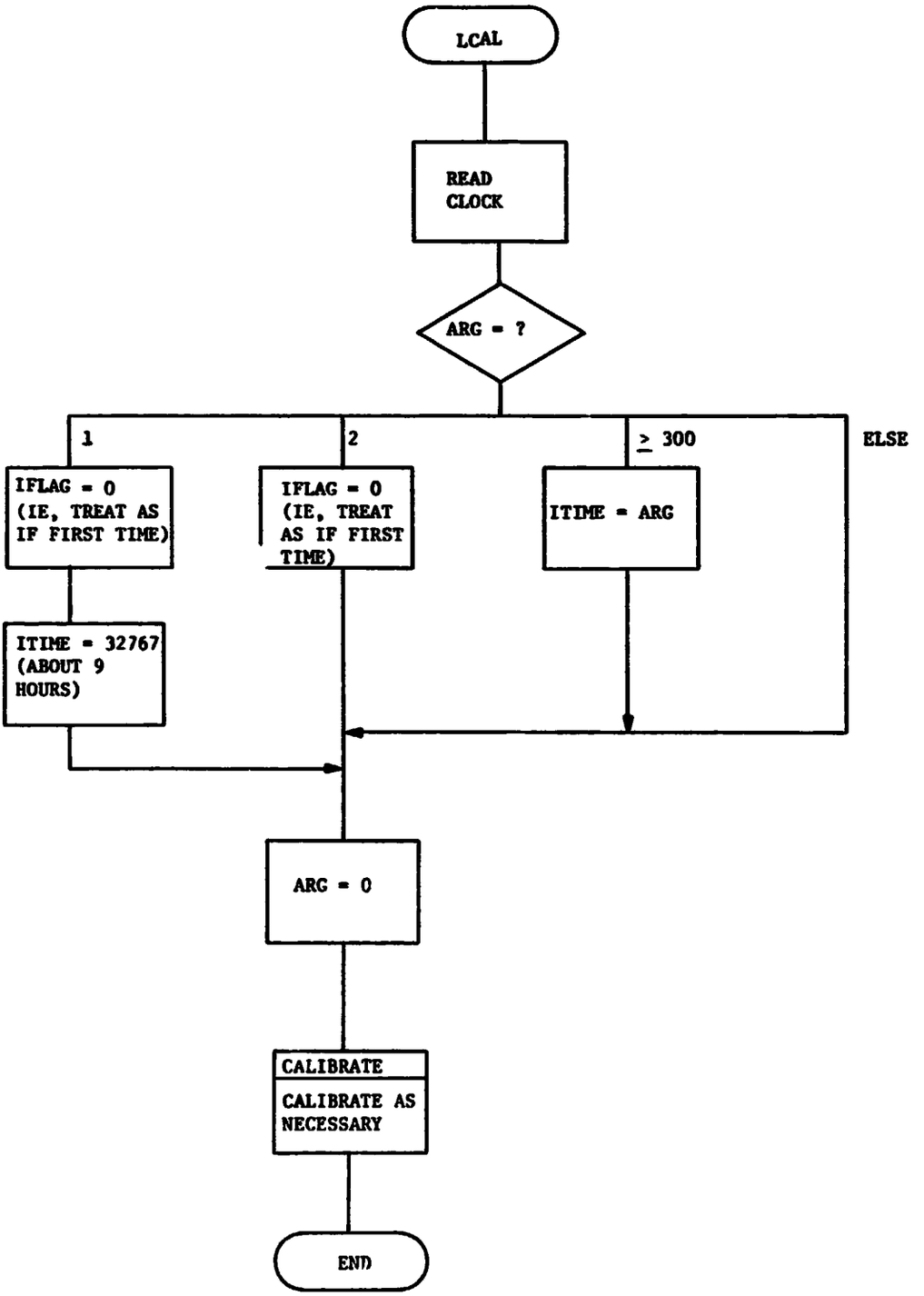
LCAL
READ CLOCK
ARG = ?
1
2
≥ 300
ELSE
IFLAG = 0 (IE, TREAT AS IF FIRST TIME)
IFLAG = 0 (IE, TREAT AS IF FIRST TIME)
ITIME = ARG
ITIME = 32767 (ABOUT 9 HOURS)
ARG = 0
CALIBRATE
CALIBRATE AS NECESSARY
END

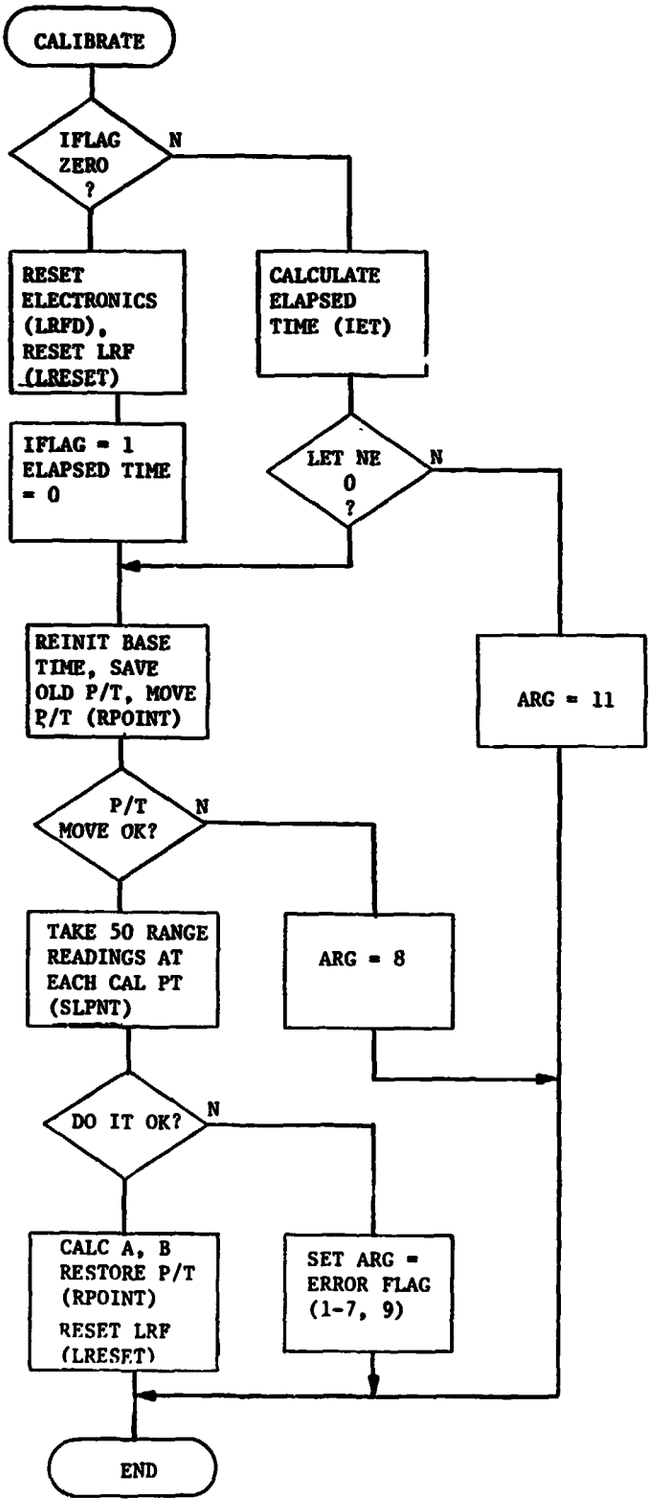
CALIBRATE
IFLAG ZERO ?
N
RESET ELECTRONICS (LRFD), RESET LRF (LRESET)
IFLAG = 1 ELAPSED TIME = 0
CALCULATE ELAPSED TIME (IET)
LET NE 0 ?
N
REINIT BASE TIME, SAVE OLD P/T, MOVE P/T (RPOINT)
ARG = 11
P/T MOVE OK?
N
TAKE 50 RANGE READINGS AT EACH CAL PT (SLPNT)
ARG = 8
DO IT OK?
N
CALC A, B RESTORE P/T (RPOINT) RESET LRF (LRESET)
SET ARG = ERROR FLAG (1-7, 9)
END

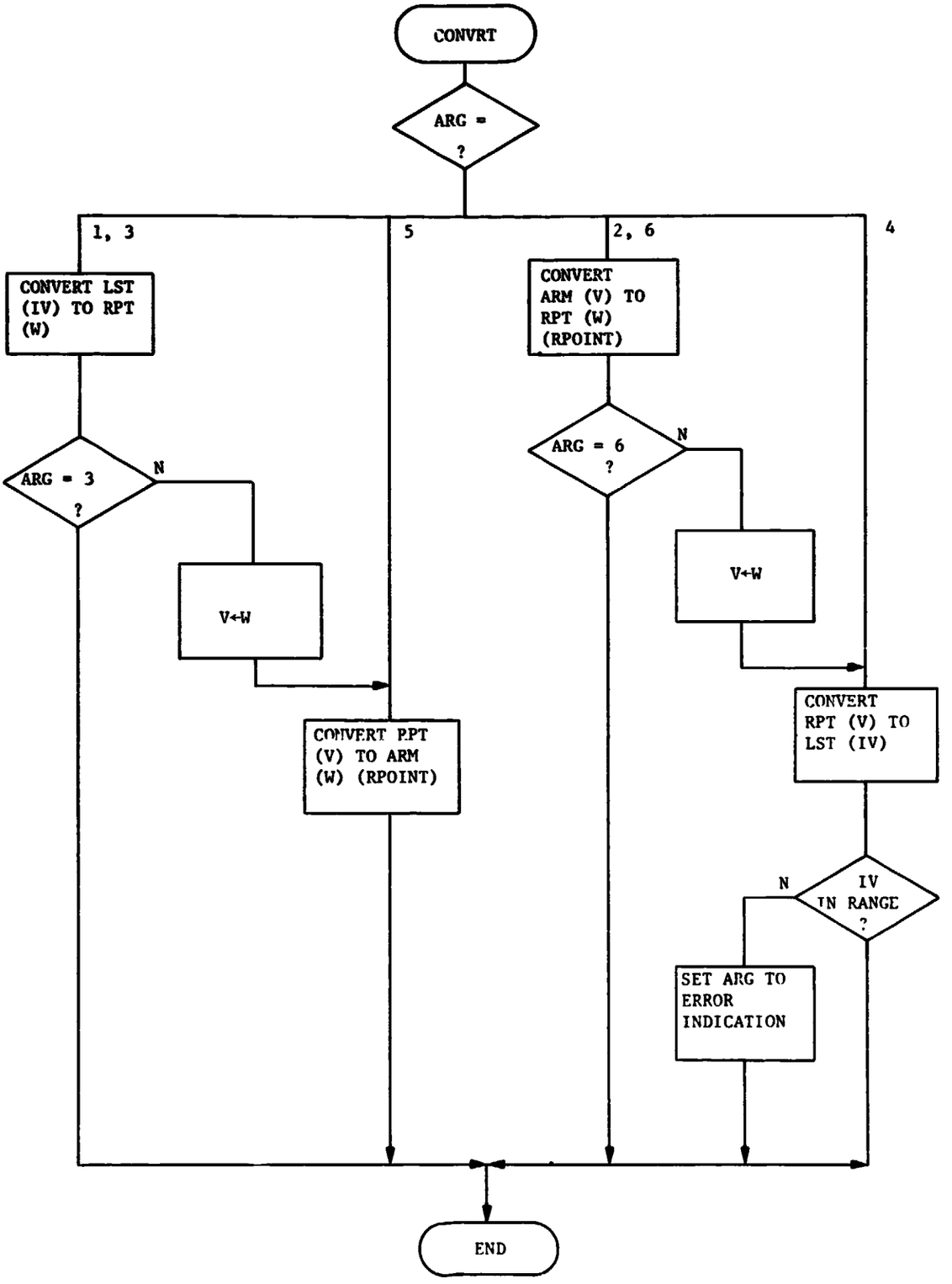
CONVRT
ARG = ?
1, 3
5
2, 6
4
CONVERT LST (IV) TO RPT (W)
ARG = 3 ?
N
V←W
CONVERT RPT (V) TO ARM (W) (RPOINT)
CONVERT ARM (V) TO RPT (W) (RPOINT)
ARG = 6 ?
N
V←W
CONVERT RPT (V) TO LST (IV)
N
IV IN RANGE ?
SET ARG TO ERROR INDICATION
END

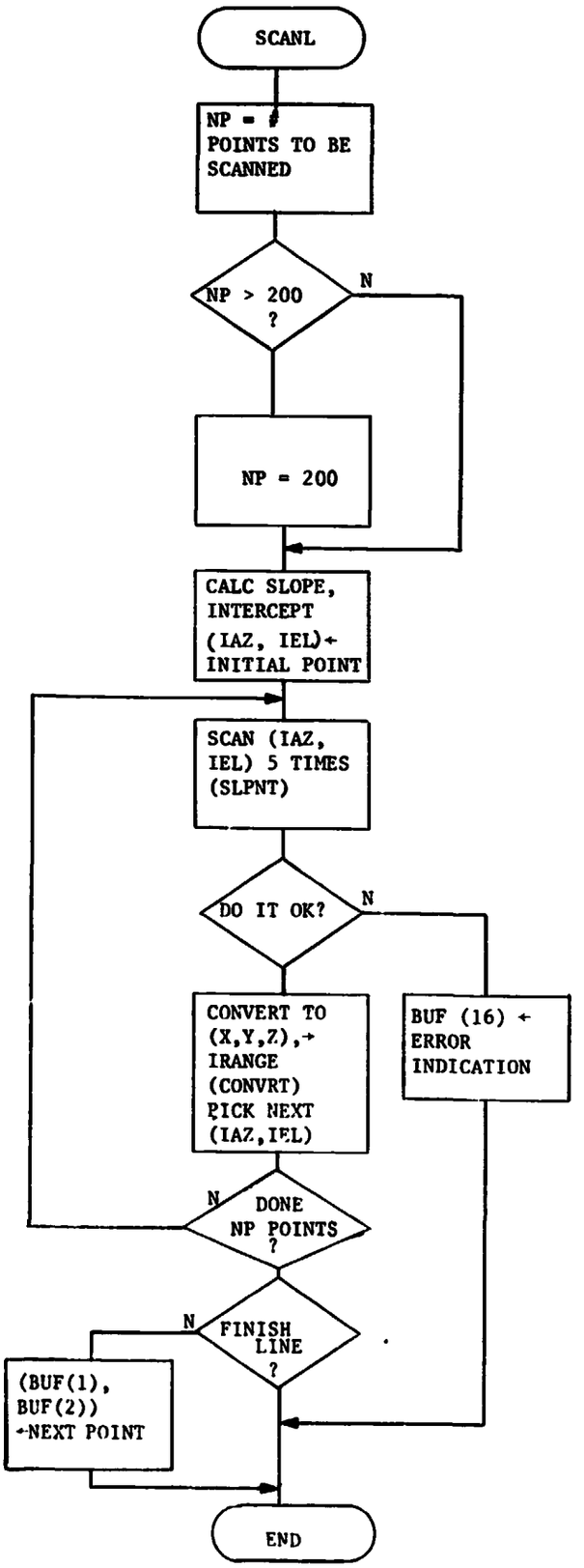
SCANL
NP = # POINTS TO BE SCANNED
NP > 200 ?
N
NP = 200
CALC SLOPE, INTERCEPT (IAZ, IEL)← INITIAL POINT
SCAN (IAZ, IEL) 5 TIMES (SLPNT)
DO IT OK?
N
CONVERT TO (X,Y,Z),→ IRANGE (CONVRT) PICK NEXT (IAZ,IEL)
BUF (16) ← ERROR INDICATION
N
DONE NP POINTS ?
N
FINISH LINE ?
(BUF(1), BUF(2)) ←NEXT POINT
END

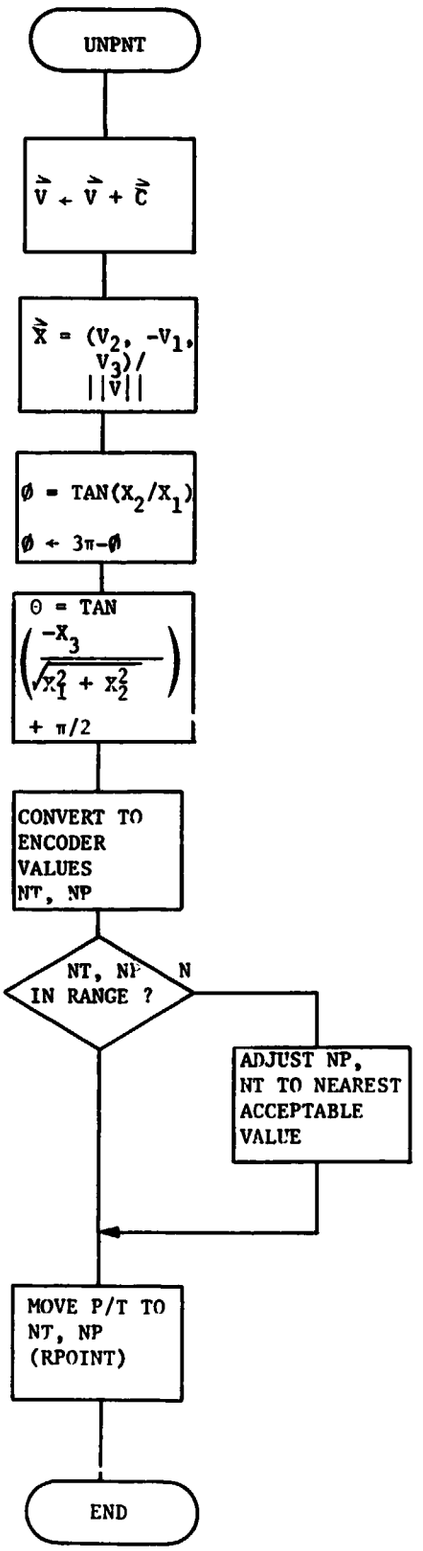
UNPNT
$\vec{V} \leftarrow \vec{V} + \vec{C}$
$\vec{X} = (V_2, -V_1, V_3)/||\vec{V}||$
$\phi = \tan(X_2/X_1)$
$\phi \leftarrow 3\pi - \phi$
$\theta = \tan\left(\frac{-X_3}{\sqrt{X_1^2 + X_2^2}}\right) + \pi/2$
CONVERT TO ENCODER VALUES NT, NP
NT, NP IN RANGE ?
N
ADJUST NP, NT TO NEAREST ACCEPTABLE VALUE
MOVE P/T TO NT, NP (RPOINT)
END

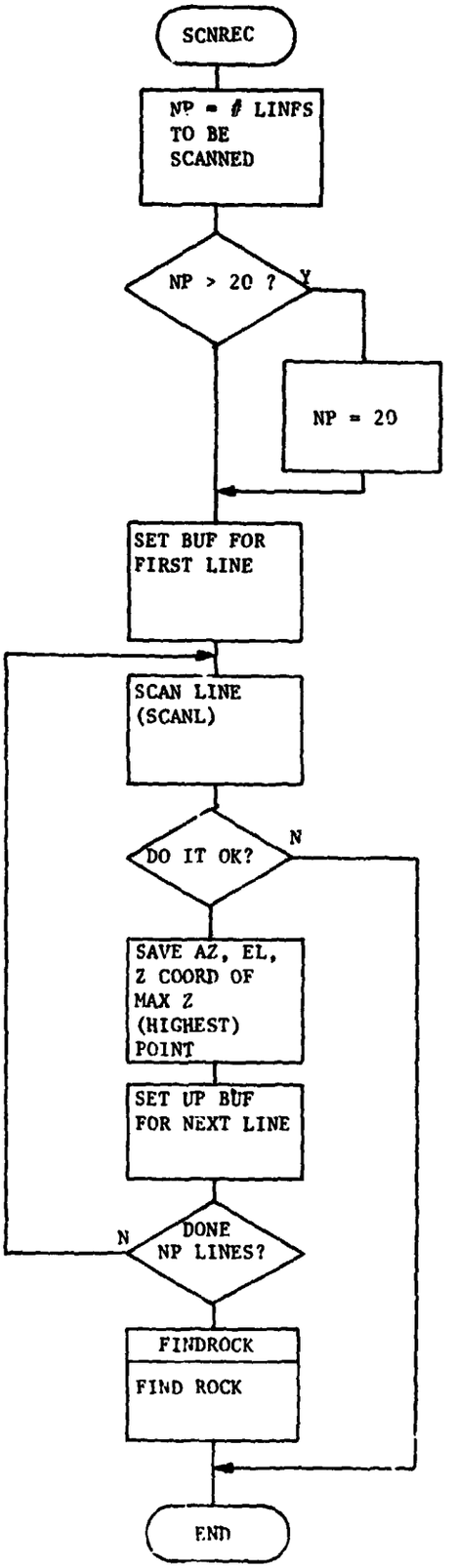
SCNREC
NP = # LINES TO BE SCANNED
NP > 20 ?
Y
NP = 20
SET BUF FOR FIRST LINE
SCAN LINE (SCANL)
DO IT OK?
N
SAVE AZ, EL, Z COORD OF MAX Z (HIGHEST) POINT
SET UP BUF FOR NEXT LINE
DONE NP LINES?
N
FINDROCK
FIND ROCK
END

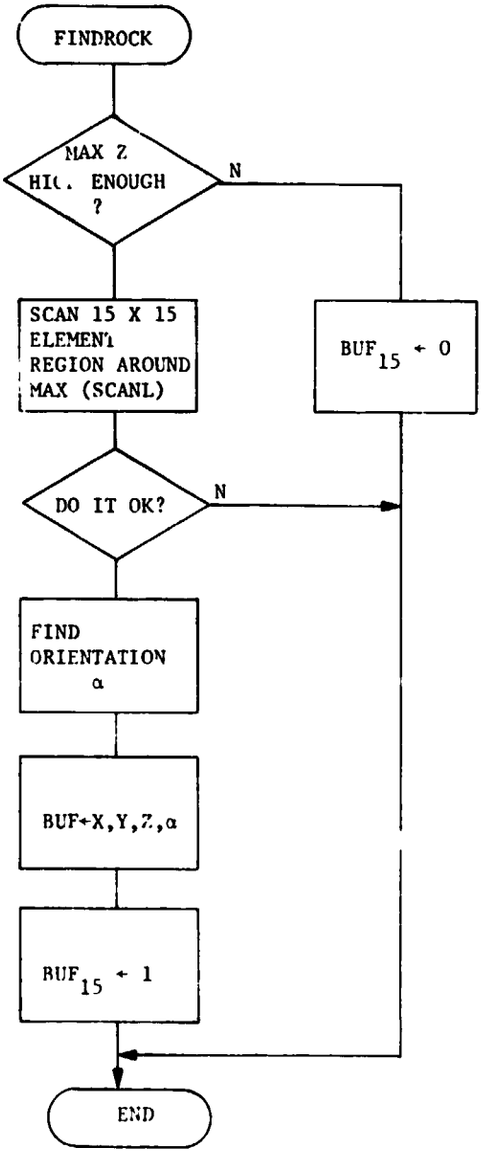
FINDROCK
MAX Z HIGH ENOUGH ?
N
SCAN 15 X 15 ELEMENT REGION AROUND MAX (SCANL)
BUF15 ← 0
DO IT OK?
N
FIND ORIENTATION α
BUF←X,Y,Z,α
BUF15 ← 1
END